Geoscience Frontiers 11 (2020) 999–1023

HOSTED BY

ELSEVIER

Contents lists available at ScienceDirect

Geoscience Frontiers

journal homepage: www.elsevier.com/locate/gsf

Research Paper

3D model of Svecofennian Accretionary Orogen and Karelia Craton based on geology, reflection seismics, magnetotellurics and density modelling: Geodynamic speculations

Michael V. Mints[a,*], Victor N. Glaznev[b], Olga M. Muravina[b], Elena Yu Sokolova[c,d]

[a] Geological Institute, RAS, Moscow, Russia
[b] Voronezh State University, Voronezh, Russia
[c] Schmidt Institute of Physics of the Earth, RAS, Moscow, Russia
[d] All-Russian Research Geological Oil Institute, Moscow, Russia

A R T I C L E I N F O

Handling Editor: Inna Safonova

Keywords:
Reflection seismics
Magnetotellurics
Svecofennian accretionary Orogen
Svecofennian Ocean
3D crustal model
Velocity-density layering

A B S T R A C T

A 3D model of deep crustal structure of the Archaean Karelia Craton and late Palaeoproterozoic Svecofennian Accretionary Orogen including the boundary zone is presented. The model is based on the combination of data from geological mapping and reflection seismic studies, along profiles 1-EU, 4B, FIRE-1-2a-2 and FIRE-3-3a, and uses results of magnetotelluric soundings in southern Finland and northern Karelia. A seismogeological model of the crust and crust–mantle boundary is compared with a model of subhorizontal velocity-density layering of the crust. The TTG-type crust of the Palaeoarchaean and Mesoarchaean microcontinents within the Karelia Craton and the Belomorian Province are separated by gently dipping greenstone belts, at least some of which are palaeosutures. The structure of the crust was determined mainly by Palaeoproterozoic tectonism in the intracontinental settings modified by a strong collisional compression at the end of the Palaeoproterozoic. New insights into structure, origin and evolution of the Svecofennian Orogen are provided. The accretionary complex is characterized by inclined tectonic layering: the tectonic sheets, ~15 km thick, are composed of volcanic-sedimentary rocks, including electro-conductive graphite-bearing sedimentary rocks, and electro-resistive granitoids, which plunge monotonously and consecutively eastward. Upon reaching the level of the lower crust, the tectonic sheets of the accretionary complex lose their distinct outlines. In the seismic reflection pattern they are replaced by a uniform acoustically translucent medium, where separate sheets can only be traced fragmentarily. The crust–mantle boundary bears a diffuse character: the transition from crust to mantle is recorded by the disappearance of the vaguely drawn boundaries of the tectonic sheets and in the gradual transition of acoustically homogeneous and translucent lower crust into transparent mantle. Under the effect of endogenic heat flow, the accretionary complex underwent high-temperature metamorphism and partial melting. Blurring of the rock contacts, which in the initial state created contrasts of acoustic impedance, was caused by partial melting and mixing of melts. The 3D model is used as a starting point for the evolutionary model of the Svecofennian Accretionary Orogen and for determination of its place in the history of the Palaeoproterozoic Lauro-Russian intracontinental orogeny, which encompassed a predominant part of the territory of Lauroscandia, a palaeocontinent combining North American and East European cratons. The model includes three stages in the evolution of the Lauro-Russian Orogen (~2.5, 2.2–2.1 and 1.95–1.87 Ga). The main feature of the Palaeoproterozoic evolution of the accretionary Svecofennian Orogen and Lauroscandia as a whole lay in the causal link with evolution of a superplume, which initiated plate-tectonic events. The Svecofennian–Pre-Labradorian palaeo-ocean originated in the superplume axial zone; the accretionary orogens were formed along both continental margins due to closure of the palaeo-ocean.

* Corresponding author.
E-mail address: gin@ginras.ru (M.V. Mints).
Peer-review under responsibility of China University of Geosciences (Beijing).

https://doi.org/10.1016/j.gsf.2019.10.003
Received 13 February 2019; Received in revised form 28 August 2019; Accepted 8 October 2019
Available online 6 November 2019

1. Introduction

Research into the deep crustal structure of the eastern Fennoscandian Shield based on the common midpoint (CMP) reflection seismic profiling along the 1-EU geotraverse and 4B cross-traverse in Russian territory was completed in 2008 (Mints et al., 2010, 2015). At the same time, similar studies were carried out under the Finnish Reflection Experiment (FIRE) project in the southeastern Fennoscandian Shield (Lahtinen et al., 2005, 2009; Kontinen and Paavola, 2006; Korja et al., 2006a, b; Kukkonen and Lahtinen, 2006). Areas in southeastern Fennoscandia divided by the Finish-Russian political border belong to the same Early Precambrian geotectonic province; the objectives and methods of both studies were similar, nevertheless the results obtained suggest only a partial joint interpretation (Mints et al., 1998). The magnetotelluric data available and obtained recently after seismic experiments in southern Finland (Korja et al., 2002; Vaittinen et al., 2012) and Karelia (Cherevatova, 2010) significantly expanded possibilities to reconstruct the rock composition in the middle and lower crust. The purpose of this work lies in the elucidation of a combined 3D seismogeological model of the Archaean Karelia Craton and late Palaeoproterozoic Svecofennian Accretionary Orogen deep crustal structure (including the boundary zone) based on methodical approaches and techniques applied earlier to deep crustal studies in the Russian part of the Fennoscandian Shield and basement of the East European Platform (Mints et al., 2009, 2010, 2015). Our study is also aimed at establishing the nature of the structural and compositional layering of the crust, Moho discontinuity and crust–mantle boundary. The seismogeological model of the crust and crust–mantle boundary is compared with a model of subhorizontal velocity-density

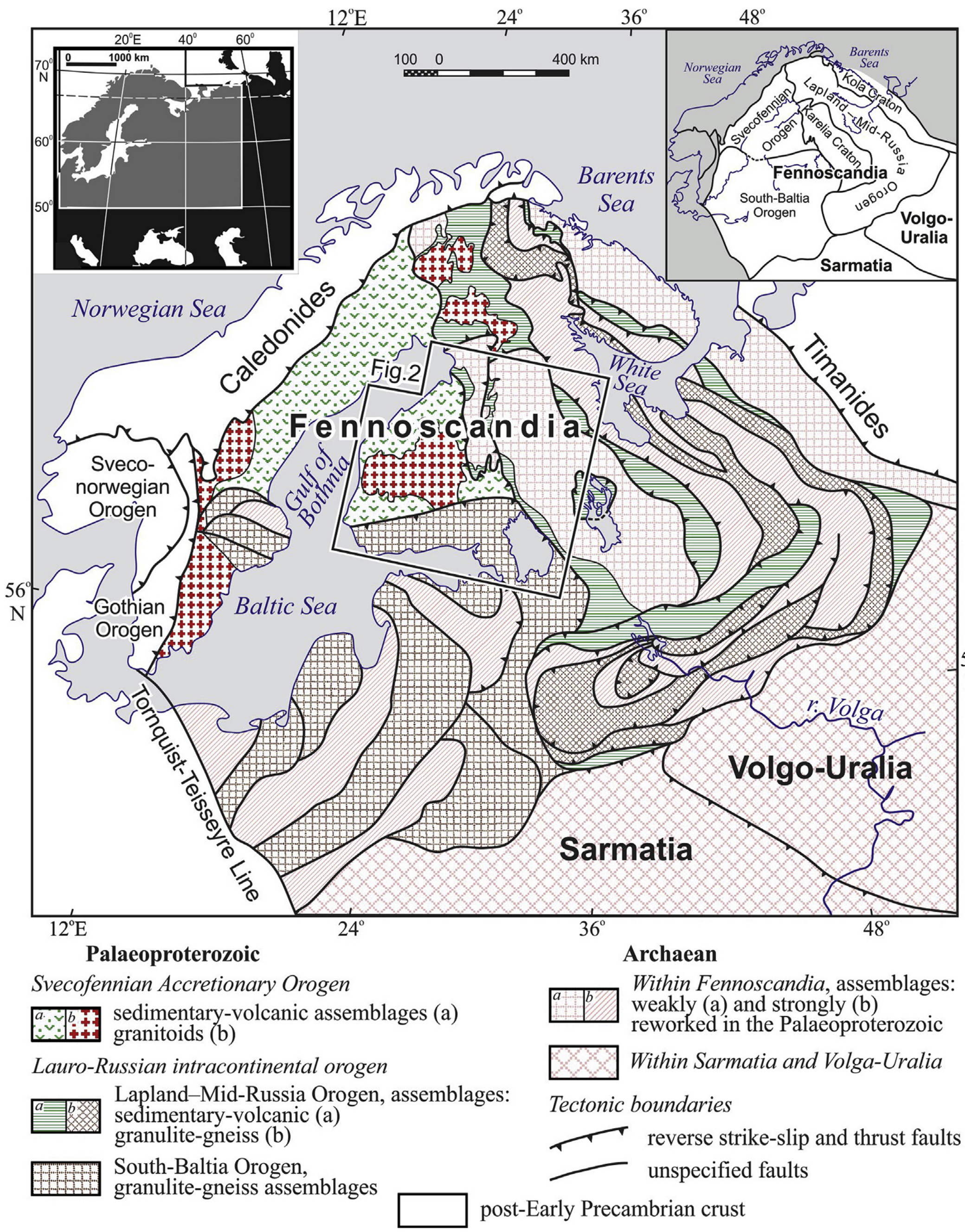

Fig. 1. Early Precambrian tectonic units of Fennoscandia based on Mints et al. (2010, 2015). Three-segment configuration of the East European Craton based on Bogdanova (1993).

layering (Glaznev et al., 2015). The final goal of our research is the development of an evolutionary model for the Svecofennian Orogen taking into account results of the deep crustal study. All experimental data that we used in our models were obtained and published earlier (see references).

2. Geological overview

Long-term geological studies led to postulation of a number of models representing the tectonic structure of the crystalline basement of the East European Platform (EEP). In recent literature devoted to regional structure and evolution of the EEP, the currently most widely adopted scheme is a three-segment configuration of the East European Craton (EEC) that forms the EEP basement, suggested by Bogdanova over two decades ago (1993). According to this scheme, the Archaean EEC's major constituents are the lithospheric segments (or the crustal segments in another version): Fennoscandia, Sarmatia, and Volgo-Uralia (Fig. 1). Further, by the end of the Palaeoproterozoic, the main features of the present-day tectonic structure of the Early Precambrian crust in the Fennoscandian Shield and in the EEC as a whole had been formed. Thus, the EEC is a Palaeoproterozoic accretionary–collisional orogen, where boundaries between major tectonic units are of Palaeoproterozoic age. These boundaries separate Palaeoproterozoic orogens and Archaean crustal domains that were relatively passive during Palaeoproterozoic orogenic events. Correspondingly, the EEC is a composite tectonic unit (for the sake of brevity, the word 'composite' is omitted below). The EEC is a part of Lauroscandia, a palaeocontinent once combining North American and East European cratons (Mints, 2007, 2013; Mints and Eriksson, 2016). In turn, a predominant part of Lauroscandia was involved in the Palaeoproterozoic Lauro-Russian intracontinental orogeny. The Palaeoproterozoic orogens are largely composed of juvenile lithotectonic assemblages, and partly of Archaean rocks, that were variably deformed, metamorphosed, and tectonically displaced. The area of our research embraces the adjacent tectonic units in the southeastern Fennoscandian Shield: the Archaean Karelia Craton and the late Palaeoproterozoic Svecofennian Accretionary Orogen, both are situated in Russia and Finland (Figs. 2, 3). The volcanic-sedimentary and volcanic-plutonic complexes of the Svecofennian Orogen border the Karelia Craton along its southwestern margin.

2.1. The Archaean: Karelia Craton and Belomorian Tectonic province

The Karelia Craton consists of the Archaean granite–greenstone domains (GGD), which are considered to be fragments of ancient microcontinents (Mints et al., 2015, Chapter 2 and references therein). Granitoids and tonalite-tronjemite-granodiorite (TTG) gneisses of the Ranua, Iisalmi, Vodlozero and Khetolamba GGDs are 3.14–2.82 Ga with a protolith age of 3.7–3.5 Ga. The tonalite–granodiorite bodies within Kianta and Kuhmo–Segozero GGDs are 2.89–2.72 Ga. The Archaean greenstone belts represent two groups. Mafic and ultramafic metavolcanics are predominant in belts of the first group. These extended linear belts are regarded as fragments of the Archaean sutures, which mark zones of microcontinent collisions (Slabunov et al., 2006; Mints et al., 2009, 2010, 2015; Hölttä, 2012; Hölttä et al., 2014). Greenstone belts of the second group are mainly composed of epicontinental metasedimentary and metavolcanic rocks dated at 2.75–2.73 Ga.

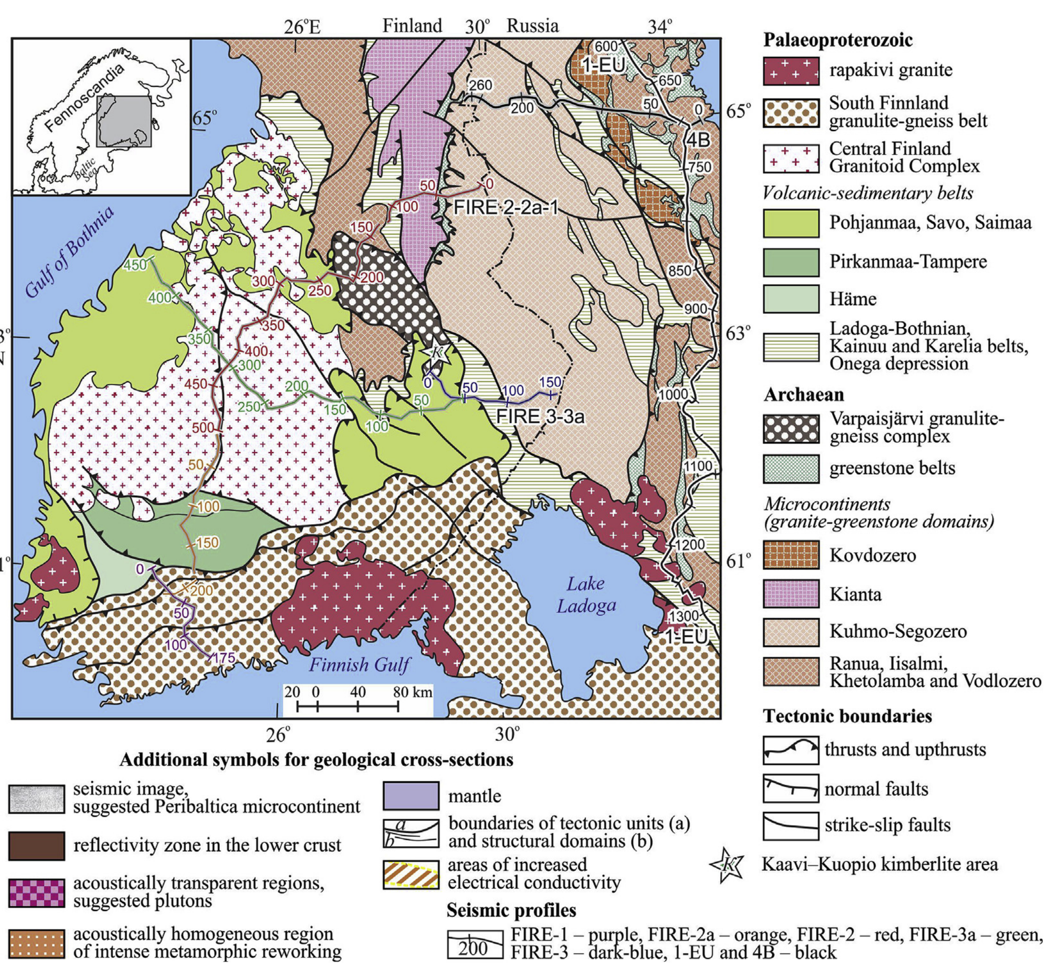

Fig. 2. Geological map of the southeastern Fennoscandian Shield (sedimentary cover removed).

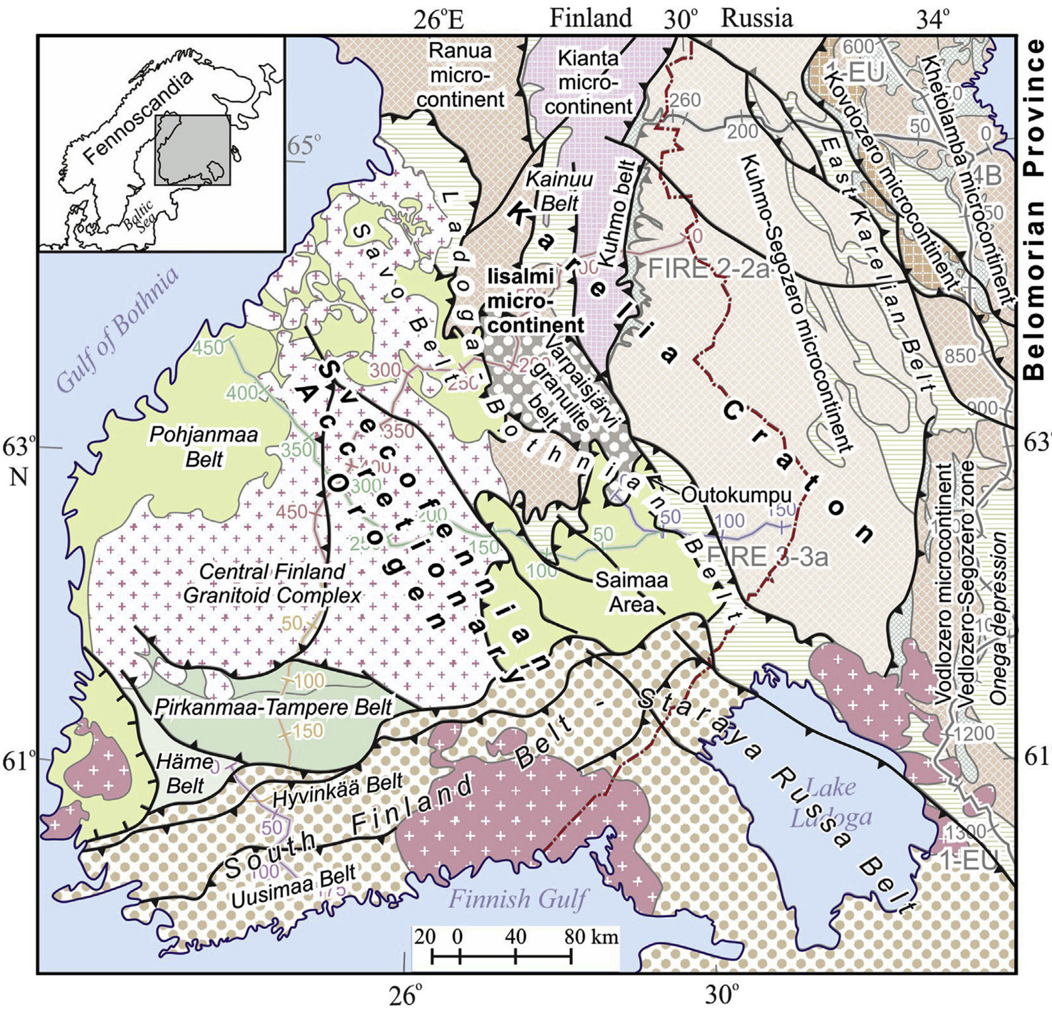

Fig. 3. Tectonic zoning of the Precambrian crust in the southeastern Fennoscandian Shield (see Fig. 2 for legend). Names of the Archaean units appear in Arial normal, names of the Palaeoproterozoic units appear in Arial italics.

The Belomorian tectonic province between the Karelia and Kola Cratons is distinguished by intensely repeated deformation accompanied by the high- and moderate-pressure metamorphism that occurred in both the Neoarchaean and Palaeoproterozoic. The Khetolamba micro-continent (granite-greenstone domain, >2.83–2.66 Ga) is the main constituent of the Belomorian province (Glebovitsky, 2005; Miller et al., 2005; Mints et al., 2010, 2015). The Kovdozero microcontinent (the Kovda–Tiksheozero thrust nappe in Mints et al. (2009)) separates the Khetolamba microcontinent and Karelia craton at the present-day surface. It is formed by TTG granitoids and gneisses hosting metasediments and metavolcanics of several greenstone belts that were originated from ca. 2.90 Ga to 2.77 Ga. The Keret' tectonic unit sandwiched between Khetolamba and Inari–Kola microcontinents contains ca. 2.89–2.70 Ga TTG gneisses and greenstones. Within Keret' gneisses, multiple subduction type eclogite bodies are distributed. We suggest that association of TTG gneisses and eclogite facies rocks is compatible with interpretation as a remnant of the Meso–Neoarchaean active margin (Mints et al., 2010, 2014, 2015).

Formation of the Karelia Craton and the Kola–Karelia palaeocontinent as a whole, including the Belomorian province, was completed in the Neoarchaean somewhat before 2.76 Ga. The later tectono-thermal events occurred under intracontinental conditions as a result of mantle-plume type processes. Specific areas of plume type thermal and tectonic activity have been identified recently in the eastern Fennoscandian Shield (Mints et al., 2015, Chapter 3). The oval-shaped Karelian–Belomorian area incorporates two main zones: (1) the central oval zone (Karelia Craton proper) is characterized by the early manifestation of tectono-magmatic and thermal activity expressed in granulite-gneiss complexes, epicontinental greenstone belts and sanukitoid massifs (2.76–2.70 Ga); (2) the arcuate zone formed by the Varpaisjärvi (Fig. 3), Pudasjärvi and Notozero-Chupa granulite-gneiss belts that is about 600 km long and has a larger radius. Granulite facies metamorphism is dated at 2.70–2.62 Ga (Mints et al., 2015, Chapter 3 and references therein).

2.2. The Palaeoproterozoic: volcanic-sedimentary belts and mafic underplating

At the onset of the Palaeoproterozoic at ~2.5–2.3 Ga, as a result of resumption of mantle-plume activity, significant volumes of mafic magma formed intrusive gabbro–anorthosite bodies at the base of the Archaean crust, whose thickness reached 60–70 km at that time. Together with host Archaean rocks, these bodies were affected by granulite facies metamorphism. In the course of subsequent late Palaeoproterozoic tectonic compression and formation of intracontinental orogens, the fragments of gabbro–anorthosite bodies were moved towards the upper crust, making up a lower portion of the tectono-stratigraphic sections of granulite-gneiss belts (gabbro-anorthosites at the base of the Lapland and Kolvitsa–Umba belts in Kola Peninsula are the best known example), whereas a predominant part of the gabbro-anorthosites were left at depth at the crust–mantle boundary (Mints et al., 2015, Chapter 8 and references therein).

The next peak of Palaeoproterozoic mantle-plume activity is dated at

~2.2–1.8 Ga. The extended rifts, which were later transformed into greenstone belts, filled with sediments, basalt and basaltic andesite lavas were formed in the inner domain of the Karelia Craton (Mints et al., 2015, Chapter 8). Extension was accompanied by local transitions from rifting to spreading and partial rupture of the continental lithosphere, in particular along the boundary between the Kuhmo–Segozero and Kianta granite–greenstone domains (Figs. 2, 3). An extensional tectonic setting at ca. 2.1 Ga was accompanied by formation of MORB-type dikes (Stepanova et al., 2014). The Jormua ophiolite complex emplaced at 1.97–1.95 Ga within the Kainuu Belt records rupture of the continental crust and the transitory existence of an oceanic structural unit of the Red Sea type (Peltonen et al., 1998).

The manifestations of areal Palaeoproterozoic mafic–ultramafic magmatism in the east of the Fennoscandian Shield and in the basement of the Moscow Syneclise on the Russian Platform coincide with those intervals of the reflection seismic profiles, where seismic images display a reflectivity zone at the base of crust. This coincidence permits interpretation of the reflectivity zone as an area of Palaeoproterozoic mantle-derived mafic magma underplating (Mints, 2011; Mints et al., 2015; see references in Thybo and Artemieva, 2013). It is of prime importance that division of the Archaean Lauroscandia continent (Mints, 2007, 2013; Mints and Eriksson, 2016) into two parts, the North American and the East European continents (cratons), accompanied by the origin of the Svecofennian Ocean are related to the same, ~2.2–1.8 Ga peak of mantle-plume type endogenic activity (Mints, 2007, 2013, 2018; Mints and Afonina, 2018). The accretionary orogen formed by closure of the Svecofennian Ocean occupies the central part of the Fennoscandian Shield.

The Neoarchaean passive margin of the Karelia Craton is overlapped with metamorphosed volcanic-sedimentary assemblages formed in shelf and continental slope settings. We regard rocks of passive margin affinity to equate to the Ladoga–Bothnian Belt, the width of which varies from 20 km to 50 km. At the base of the preserved passive margin, the middle and upper Palaeoproterozoic stratified rocks are distributed fragmentarily. In the lower part of the sedimentary succession, quartzite and quartzitic sandstone are combined with basal conglomerate and gravelstone, which often overlie directly the Archaean basement. Variegated dolomite and limestone with subordinate sandstone and shale follow up the succession. The upper part of the succession is composed of biotite–quartz schists, frequently sulphide- and graphite-bearing with participation of carbonate rocks and quartzite. Graphite occurrences and deposits are related to graphite-bearing rocks: the Kitela deposit and a group of occurrences in the northern Ladoga region; the Viistola deposit in Finland (Biske and Kolodey, 2014; Gautneb et al., 2016). The Sortavala and Ladoga groups occur up the section. These comprise amphibolite (metatholeiite) with participation of biotite, biotite–garnet gneisses (metavolcanic rocks of andesitic and dacitic compositions); dolomite and calcite marbles, calciphyre; amphibole, mica, mica–quartz schists and quartzites, as a rule, enriched in sulphides and graphite; andalusite-staurolite, sillimanite–two-mica, and cordierite gneisses (metasandstones and metasiltstones). Sedimentation on the shelf of the passive margin started at about 2.0 Ga and continued up to 1.91 Ga (Huhma et al., 1991). During formation of the Svecofennian Accretionary Orogen, these complexes were thrust northeastward over the craton margin.

2.3. The Palaeoproterozoic: Svecofennian Accretionary Orogen

The southeastern part of the Svecofennian Accretionary Orogen exposed in Finland is composed of volcanic-sedimentary belts and granitoid massifs (Pajunen et al., 2008; Nironen, 2017). The Savo Belt, Outokumpu, and Saimaa domains are adjacent to the Karelia Craton in the east. Further to the southwest the Central Finland Granitoid Complex (CFGC) embraces the predominant part of southern Finland. In the west the CFGC borders on the Pohjanmaa Belt, in the southwest there are the Pirkanmaa-Tampere and Häme belts (Figs. 2, 3).

The Savo Belt 60–70 km in width extends along the boundary with the Karelia Craton. It is composed of intercalating weakly and moderately metamorphosed graywacke, chert, sandstone, and in areas of more intense metamorphism of micaceous, graphite- and/or sulphide-bearing schists and paragneisses, including several graphite occurrences (Gautneb et al., 2016) with interlayers of 1.93–1.92 Ga amphibolites and gneisses (metavolcanic rocks). About half of the belt is occupied by granitoid massifs formed at 1.91–1.88 Ga and 1.88–1.87 Ga. The Savo Belt is commonly considered as a fragment of primitive island arc (Korsman et al., 1997; Lahtinen et al., 2005).

An oval domain (in plan view), about 100 km in diameter constitutes the southeastern continuation of the Savo Belt. This domain contains the Outokumpu and Saimaa areas, which are composed of similar rocks to the Savo Belt; however, the abundance of granitoids is lower and the metasedimentary rocks are noticeably predominant. Restricted occurrences of mafic metavolcanics associated with serpentinite are regarded as the Outokumpu ophiolitic complex, which is obducted on to the margin of the Karelia Craton. A deposit of Au-bearing Cu–Co–Zn sulphide ore is related to the Outokumpu ophiolites (Kontinen, 1988; Sorjonen-Ward et al., 2004). It is suggested that the Outokumpu ophiolitic complex was formed at the initial stage of oceanic basin opening, which followed breakup of the Karelia Craton at about 1.97 Ga (Huhma, 1986). The mineralization was formed in the oceanic environment at 1.95 Ga. Afterward, during closure of the ocean and the 1.90 Ga collision of an island arc, the ophiolitic complex was squeezed westward over the margin of the Karelia Craton (Lahtinen et al., 2005; Kontinen et al., 2006).

The Pohjanmaa (Pyhäsalmi) Belt in southwestern Finland represents a depression, approximately oval in shape and about 180 km in extent. It is filled with metasedimentary rocks: graywacke, quartzite, sandstone, mica schist, graphite- or sulphide-bearing schist and paragneiss with lenses and interlayers of amphibolite (mafic metavolcanic rock) that were deposited at 1.90–1.87 Ga in a backarc or interarc basin (Koistinen et al., 1996, 2001; Rutland et al., 2004; Lahtinen et al., 2005). The near-latitudinal Tampere Schist Belt, more than 100 km in extent, is formed of 1.90–1.89 Ga metasedimentary and island-arc type felsic, basic, and intermediate metavolcanic rocks (Koistinen et al., 2001; Lahtinen et al., 2005). The lower part of this section consists of mafic lavas erupted in a riftogenic or backarc setting no later than 1.90 Ga (Kähkönen, 1989; Huhma et al., 1991; Lahtinen et al., 2002). The volcanic-sedimentary sequence is intruded by granitoid bodies related to the CFGC. The lower part of the tectono-stratigraphic section in the southern part of the belt consists of turbidites and clay-rich sedimentary rocks enriched in graphite and sulphides that is not characteristic for the rest of the belt (Kähkönen, 1999). The Pirkanmaa Belt, 175 km in extent, may be regarded as the southern constituent of the Tampere Belt. In contrast to the Tampere Belt, metasedimentary rocks (metagraywacke, chert, metasandstone, micaceous schist, graphite- and sulphide-bearing schists) are predominant, whereas metavolcanic rocks play a subordinate role. Graphite occurrences are known in the western part of the belt (Gautneb et al., 2016). The Häme volcanic-sedimentary belt is cut through by granitoid massifs and minor bodies of gabbro, diorite, and ultramafic rocks. The southern segment of the belt is overlapped by a tectonic nappe of the South Finland granulite–gneiss belt (in our understanding, see Mints et al., 2015, (Chapter 8).

The CFGC covers 40,000 km^2 and lies in the centre of southern Finland. The thickness of the sill-shaped body intersection by the FIRE-1, FIRE-2 and FIRE-3 profiles is ca. 10 km, according to the geological interpretation in Korja and Heikkinen (2008). The CFGC makes up an important, but so far still insufficiently studied constituent of the Svecofennian Orogen. Isotopic geochronological data provide evidence for a ~2.1–2.0 Ga crustal source (Lahtinen and Huhma, 1997; Rämö et al., 2001; Lahtinen et al., 2015). Synorogenic calc-alkaline granodiorite, tonalite, granite, monzonite, syenite, and their metamorphic proxies dated at 1.89–1.87 Ga (Lahtinen and Huhma, 1997 and references therein) are predominant in the complex. They are subdivided into synkinematic (~1.89–1.88 Ga) and postkinematic (~1.88–1.87 Ga) groups, which differ in geological relationships, geochemistry, and petrography (Nironen et al., 2000; Rämö et al., 2001). Postkinematic granitoids display attributes of bimodal (mafic–felsic) magmatic association typical of extension settings. The petrologic (Elliott et al., 1998) and geochemical (Art et al., 1978; Nironen et al., 2000; Nikkilä et al., 2016) data showed that postkinematic granite crystallized from dry high-temperature A-type magmas and/or magmas of the charnockite–enderbite series (Mints et al., 1996).

In various places within the Svecofennian Orogen, zircons with ages of 2.08–1.91 Ga and of 2.78–2.45 Ga (in smaller quantities) were found in metasedimentary and igneous rocks. This implies that juvenile middle Palaeoproterozoic crust, which predated Svecofennian accretion, actually existed. This crust also incorporates Archaean fragments (Andersson et al., 2006 and references therein). The study of the Hf isotopic system in zircons from mafic intrusions in southern Sweden provides evidence for a moderately depleted mantle source (Andersson et al., 2011). Addressing other parts of the Svecofennian Orogen, this study points to the existence of proto-Svecofennian crust (<2.2–1.9 Ga), which includes a less significant Archaean component.

2.4. *The Palaeoproterozoic: intracontinental Lapland–Mid Russia–South Baltia Orogen*

The final event in the Palaeoproterozoic history of the composite East European Craton was formation of the intracontinental Lapland–Mid Russia–South Baltia Orogen (Fig. 1), which adjoins the Karelia Craton in the north, east, south, and southwest (Mints et al., 2010, 2015, Chapter 8). The South Baltia sector of the orogen comprises a sequence of belts which are arcuate in plan view, convex to the east, and which exhibit contrastingly different grades of metamorphism: greenschist–epidote-amphibolite facies in certain belts and high amphibolite to granulite facies in others. The arcuate belts are characterized by centroclinal plunging of the tectonic nappes and centrifugal thrusting over rocks of the framework. The Staraya Russa–South Finland granulite-gneiss belt (Figs. 1–3), marginal in the east, extends from Lake Il'men and the town of Staraya Russa to the north, and then further via the northern Ladoga region to the west along the northern coast of the Gulf of Finland. This belt reaches 1200 km in extent. Over the entire history of geological study of Finland, the South Finland branch of the Staraya Russa–South Finland Granulite-Gneiss Belt was regarded as a structural element of the Svecofennian Orogen proper. It was usually called the South Finland volcanic-sedimentary complex, however, some authors used other terms (Korsman et al., 1999; Väisänen et al., 2000; Lahtinen et al., 2005; Korja et al., 2006b). In the papers of Finnish researchers, the rocks making up the belt are combined into volcanic-sedimentary associations intruded by late orogenic granitoids, e.g., in Rämö et al. (2001). Metamorphism is envisaged only as a circumstance, which hampers identification of the initial composition of rocks. In the last several years, based on Kähkönen et al. (1994), it is commonly suggested that rocks of the belt were formed in the backarc basin of a mature island arc.

The outer zone (lower portion of the tectono-stratigraphic section) of the arcuate Staraya Russa–South Finland Belt is composed of hypersthene granulite-gneiss, enderbite, hypersthene granite, amphibolite, paragneiss, and migmatites. Up section, garnet–cordierite–graphite gneiss (khondalite), granite, and plagiogranite with garnet, cordierite, and graphite are predominant. In the western part of the belt, several graphite occurrences are known (Gautneb et al., 2016). In the northern Ladoga region, the belt is composed of amphibolite, amphibole and two-pyroxene–plagioclase schists; biotite, biotite garnet, biotite–cordierite, and biotite–sillimanite–cordierite gneisses (Koistinen et al., 2001; Glebovitsky, 2005). The Ikhal'sky deposit of coarse- and medium-flaky graphite is located in this part of the belt (Biske and Kolodey, 2014). In rocks of the paraautochthone, composed of the Sortavala Group, the inverted metamorphic zoning is characterized by parameters of metamorphism from 550 °C near the granulite nappe border to 450 °C at a distance from the latter.

In the South Finland branch of the belt, granulite and amphibolite facies schists and gneisses are predominant. These are metagraywacke, chert, metasandstone, micaceus schist, graphite- and/or sulphide-bearing schists, paragneiss, and amphibolite. The protoliths of these rocks are dated at 1.95–1.87 Ga and apparently are older than those ages (Väisänen et al., 2000; Koistinen et al., 2001; Glebovitsky, 2005). High-temperature metamorphism developed twice: at 1.89–1.87 Ga and 1.83–1.81 Ga (main orogenic and late orogenic stages according to Väisänen et al. (2000) and references therein). A significant part of the South Finland branch is occupied by granodiorite and diorite, partly hypersthene-bearing, and their metamorphosed proxies dated at 1.91–1.88 Ga. Younger granite, monzonite, syenite, monzodiorite and their metamorphosed proxies form the main component. The age of this rock group is estimated from ~1.88 Ga to 1.87 Ga (Koistinen et al., 2001); younger estimates at ca. 1.82 Ga are also noted (Väisänen et al., 2000 and references therein). The thermobarometric data give evidence for localizaton of intrusive bodies at a depth more than 15 km; the high temperature of melts corresponds to dry conditions of granulite facies. The continuation of the South Finland branch of the granulite-gneiss belt to the west is recorded in the southern part of the Bergslagen region in southern Sweden (Andersson et al., 2006). Research in the northern Ladoga domain within Russian territory yielded close age estimates of metamorphic events: the 1.88–1.85 Ga metamorphism M1 and 1.80–1.72 Ga metamorphic event M2. In the para-autochthon, inverted metamorphic zoning is observed (our interpretation of data published by Baltybaev et al., (2000, 2006) and Glebovitsky, (2005)).

It is accepted that the Karelia Craton and the Svecofennian Accretionary Orogen are divided by the Raahe–Ladoga Suture, i.e., the NW-trending steeply dipping right-lateral strike-slip fault zone, which is traced according to geological and geophysical data from the northern Ladoga region to the Skellefteå district in northern Sweden.

3. Geological interpretation of geophysical data: approaches and techniques

3.1. *Models of the crust and boundary between crust and mantle based on seismic studies in refracted and reflected waves, relationships between velocity–density and seismic-geological models*

The Moho discontinuity was discovered a century ago; however, its origin and genesis, as well as the interface between crust and mantle remain one of the main problems in studies of the lithosphere (Carbonell et al., 2013; Prodehl et al., 2013). It was accepted historically that the terms "crust–mantle boundary" and "Moho discontinuity" are synonymous, although actually this is not the case. The Moho discontinuity is a geophysical image of the virtually continuous and smoothly curving surface of global rank, characterized by more or less sharp change in compressional wave velocity from 6.9–7.4 km/s to 8.0–8.2 km/s (Christensen and Mooney, 1995). The Moho discontinuity is an averaged and smoothed image of the boundary between the Earth's crust and mantle. In turn, the "crust–mantle boundary" is an integrated geological phenomenon specified by a set of properties of the crust, upper mantle and their transitional zone, including rock composition, mechanical properties and grade of metamorphism as well as structural features of this interface.

The concept of the Moho discontinuity is an essential component of the velocity and related density models that assume the division of the crust into subhorizontal layers distinguished by composition and grade of metamorphism. It was suggested that wide-angle reflection and refraction seismic methods deliver strong evidence for increase in rock density and for the importance of metamorphic grade generally increasing with depth (e.g., Fountain and Christensen, 1989). On the basis of more than 3000 laboratory rock density measurements at high pressures in various rock samples, at pressures corresponding to the conditions in the Earth's crust, Christensen and Mooney (1995) showed that changes in density even at maximum pressures at the Moho level are relatively small. To explain the density increase with depth, accounting for these results one should assume not only a change in the composition of the rocks, but also an increase of metamorphic parameters. Besides, these measurements cannot explain density adequation of mafic and felsic rocks at crustal depth. "Velocities in the upper continental crust are matched by velocities of a large number of lithologies, including many low-grade metamorphic rocks and relatively silicic gneisses of amphibolite facies grade. In midcrustal regions, velocity gradients appear to originate from an increase in metamorphic grade, as well as a decrease in silica content. Tonalititic gneiss, granitic gneiss, and amphibolite are abundant midcrustal lithologies. … The bulk of the lower continental crust is chemically equivalent to gabbro, with velocities in agreement with laboratory measurements of mafic granulite. Garnet becomes increasingly abundant with depth, and mafic garnet granulite is the dominant rock type immediately above the Mohorovicic discontinuity" (Christensen and Mooney, 1995, p. 9761). The estimates of the composition and level of metamorphism based on the seismic velocity data as well as related rock density estimates are further introduced into deep crustal structure models (e.g., Christensen and Mooney, 1995; Abbott et al., 2013; Carbonell et al., 2013; Thybo and Artemieva, 2013). The differences in position of the refraction Moho and the reflection image of the crust–mantle boundary are noted in White et al. (2005), Cook et al. (2010) and O'Reilly and Griffin (2013). Comparing the corresponding cross-sections of three-dimensional seismogeological and velocity-density crustal models of the southeastern Fennoscandian Shield, we find that rocks of different composition, both mafics and granitoids, penetrate the high-density lower crust and reach the crust–mantle boundary. Results of our investigation demonstrate that the main features of the deep crustal structure and crust–mantle boundary, including the ensembles of overthrust-underthrust tectonic slices, are preserved for a very long time (Glaznev et al., 2015 and this work). They produce a series of inclined seismic reflections, which cannot be reconciled with subhorizontal velocity-density layering of the crust (cf. Balling, 2000).

Up to the present time, the most popular interpretation is a three-layered model of the crust subdivided into the lower, middle, and upper crust. Although these terms to a certain degree follow the model of subhorizontal crustal layering, they, however rule out a direct correlation of velocity and calculated density versus composition of the crust. These terms do not suggest distinct constraints and are convenient for description of crustal properties at various levels. The seismic wave velocity and rock density increase regularly from upper to lower crust. To denote these layers, terms are often used which indicate composition of rocks with velocity and density characteristics most closely corresponding to experimentally estimated ones for a particular layer (the so called granitic, dioritic, basaltic ones, or basic granulite layers). It should be noted that despite the conventional character of these terms (Belousov, 1960), some authors perceive them literally.

The above contradictions forced the authors to pay special attention in this article to a discussion of the nature of the Moho discontinuity and the crust–mantle boundary, and the main differences between the crustal models based on refracted and reflected seismic images.

With progress in data acquisition and processing, models of crust consisting of numerous subhorizontal layers and lenticular bodies varying in thickness, velocity, and density have been elaborated. Relying on these features, some authors attempt to identify the composition of rocks or rock associations making up particular crustal layers (e.g., Korsman et al., 1999; Mooney et al., 2002; Kozlovskaya et al., 2004; Bogdanova et al., 2006; Kuusisto et al., 2006; Janik et al., 2009; Thybo and Artemieva, 2013; Janutyte et al., 2014; Silvennoinen et al., 2014). These models do not differ from preceding models of subhorizontal layering of the crust in respect of their basic approach to geological interpretation.

The seismogeological models of the crust beneath the southeastern Fennoscandian Shield presented in Glaznev (2003) and Glaznev et al. (2015) contradicted models of rock distribution patterns characterized by different composition and metamorphic grade, similar to those presented in Christensen and Mooney (1995) and Kuusisto et al. (2006). The global experience of geological mapping does not provide examples of subhorizontal crustal boundaries at the surface. Metamorphic reactions are not able to ensure reversibile changes in the rock density when the crust is uplifted due to tectonic processes or denudation. As a result, we have to suppose the existence of some mechanism of reversible compaction of rocks with depth. Today, such a mechanism is unknown. We hope that the results of our studying the specific example of the southeastern Fennoscandian Shield will give impetus to the further investigation of this mechanism.

We specifically discuss the horizontal and non-lithostatic deviations from the regular density layering discussed by Mints et al. (1998) and Glaznev et al. (2015). In particular, it showed that subhorizontal density layering of the crust is superimposed on the previously formed geological structure; the density differentiation of the crustal rocks decreases with depth; the morphological peculiarities of the layer boundaries are determined predominantly by the current and relatively recent state of the crust, but may be disturbed as a result of recent deformations. Seismogeological (in terms of reflection patterns) and velocity-density models exist almost independently of each other, methods of refracted and reflected seismics allow us to explore different features of the geological environment.

In 1970s–1980s, intense deep studies were undertaken in continents using reflected waves in nearly vertical beams with application of vibroseis sources. The seismic images of crust (patterns of seismic reflections) in Precambrian cratons display wide variations of structural characteristics and emphasize the determinant role of inclined reflections. The seismic images of the boundary between the Precambrian crust and mantle are widely variable and display a certain dependence on structure and genetic history of the crust. The crust–mantle boundary, as a rule, is prominently expressed as a transition from moderately or intensely reflecting lower crust to acoustically transparent mantle. In some cases, the lower crust is acoustically translucent, and the crust–mantle boundary seems to disappear, although the Moho discontinuity (based on refracted waves) remains quite distinct. Finally, cases are known where a seismic image of crust gradually gives way to acoustically transparent mantle (BABEL Working Group, 1990; Abramovitz et al., 1997; White et al., 2000; Van der Velden and Cook, 2005; Kukkonen and Lahtinen, 2006; Mints et al., 2009, 2010, 2015; Cook et al., 2010; Hammer et al., 2010; Mints, 2011, 2016). The lower crust in the seismic reflection pattern is commonly identified as a zone of multiple subhorizontal intense reflections (reflectivity zone), which in many cases, though by far not all, immediately overlies the crust–mantle boundary. The detailed review of this phenomenon was published by Mooney and Meissner (1992), where a great number of the models describing lower crustal reflections are presented and critical assessments of these models are considered. The model of layered lower crust is the most popular as a geological image of the reflectivity zone, which is formed under conditions of extension accompanied by bedding-plane intrusions of mantle-derived mafic magma (Holliger and Levander, 1994). The contrast of acoustic impedance arises along boundaries between mafic intrusions and crustal rocks.

Unlike models of the subhorizontally layered crust, which emphasize weakness or absence of interrelations between geological structures observed at the surface and deep-seated layers, the patterns of widespread inclined seismic reflectors (White et al., 2005; Kukkonen and Lahtinen, 2006; Cook et al., 2010; Hammer et al., 2010; Mints et al., 2010, 2015; Mints, 2016) may reliably be combined with geological maps in terms of 3D models (Mints et al., 2010, 2015; Mints, 2016). In turn, the 3D models of the crust, crust–mantle boundary, and upper lithospheric mantle create an essentially new basis for investigation of the lower crust and crust–mantle boundary in the basement of ancient cratons. Owing to the close links of geological features in the lower crust and the upper lithospheric mantle, as well as to the coherent lateral variations in the crust–mantle boundary structure and geological features at the surface, we have managed to create a fundamentally new basis for discussion of deep crustal structure, geodynamic settings, tectonic and thermal events in the cratons' genetic history recorded in seismic images (Mints et al., 2009, 2010, 2015).

The authors of some recent publications attempted to combine, in general model terms, the data of seismic profiling in gentle beams (velocity–density models) and in near-vertical beams (on the basis of reflected waves, structural–geological models), in particular, along some profiles of the LITHOPROBE program (Cook et al., 2010) and POLAR, HUKKA, FIRE-4 profiles in Finland (Janik et al., 2009). Evaluating the results obtained from a less conciliatory viewpoint, we suppose that these types of integrated models, in fact, represent models of subhorizontal layering, with some of the structural directions taken from the seismic reflection images being superimposed selectively.

The idea of the primary independence of models of the subhorizontally layered crust and models of geological structure relying on reflection seismic images is an alternative to such attempts (Mints et al., 1987a, b). The subhorizontal seismic velocity boundaries in the crust never reach the surface, independently of type and complexity of crustal tectonic patterns, block, fold, or thrust nappe types. This can be explained by the reasons listed below: the boundaries, formed in the consolidated crust approximately following the surface, are displaced within the crust due to subvertical tectonic motions, recovery of isostatic equilibrium, erosion of the upper part of the crust etc. Deviations from the general position of velocity layering may be results of diverse additional influences: heat and fluid flows, tectonic stress, lithostatic pressure, etc. A special discussion on two types of seismic boundaries was initiated by Glaznev et al. (2015). It showed that (1) the subhorizontal density layering of the continental crust is superimposed on the earlier geological structure; (2) the differentiation of the rock density decreases with depth, and only in the upper crust down to a depth of 5–10 km do the rocks retain their individual density; (3) the features of density layering are determined in the first degree by the present-day and relatively recent state of the crust, but may be disturbed as a result of the latest deformations; (4) the notions of the lower continental crust as a reflectivity zone and as a layer of significantly increased density and velocity are not equivalent; (5) a high level of compaction in the crust under lithostatic loading cannot be explained on the basis of relatively simple ideas on metamorphism and/or compaction of rocks inferred from laboratory study of rock samples and corresponding numerical models. This implies that additional and vigorous mechanisms exist, which ensure reversible variations of rock density (Glaznev et al., 2015).

Two rock types are predominant within the crust of the study region: (1) large bodies of low-density and low-velocity gneisses and granitoids (2.58–2.8 g/cm^3 and 5.2–6.2 km/s); and (2) high density and high-velocity amphibolites (2.8–2.9 g/cm^3 and up to 3.2 g/cm^3 and 6.0–7.2 km/s) that rank much lower in abundance and make up thin (from a few centimeters to a few meters; Berzin et al., 2001; Mints et al., 2010) lenticular bodies and layers that extend for tens and hundreds of meters (for a few kilometers occasionally). The amphibolites intercalated with amphibole and biotite-amphibole TTG gneisses are often grouped into formations, up to a few kilometers in thickness. Metamorphic and migmatite banding on limbs of large folds reveal a roughly persistent trend, resembling the general stratification of the sequence as a whole that readily deforms in compliance with the contours of large tectonic units.

The study of reflections in crust consisting of metamorphic rocks indicates that the spectacular, confidently identified packets of reflections may, in some cases, be caused by constructive interference of reflections from boundaries of relatively thin interlayers having high acoustic impedance. The thickness of particular interlayers may be only a few decimeters, i.e. approximately 1/100 to 1/300 of wavelength (Ji et al., 1997). A representative section of such a geological medium was obtained from drilling the Kola Superdeep Well that penetrated a Neoarchaean gneiss–amphibolite–migmatite sequence from a depth of 6842 m down to 12,262 m at the borehole base (Kozlovsky, 1984). The migmatized gneisses and granites make up a matrix for non-uniformly embedded interlayers of dense, high-velocity amphibolite and meta-ultramafic interlayers varying in thickness from a few meters to 15–25 m and occupying approximately 20% of the section. The synthetic gathers (time sections), calculated along the Kola Superdeep axis (Mints and Stupak, 2001; Mints et al., 2004) in order to estimate the role of thin amphibolite interlayers in the creation of the seismic reflection pattern, have demonstrated the crucial contribution of interference from thin interlayers to the reflection pattern. It was found that the degree of reflectivity within the section does not reveal a direct correlation with the number and dimension of geological bodies having petrophysical parameters that provide effective reflections at their boundaries.

In the geological interpretation of seismic data, we attached particular significance to the direct tracing of recognized geological boundaries and fault zones in reflection patterns toward the present-day surface and to their correlation with mapped geological and tectonic units. Comparison of the seismic image geometry with the geology of the eastern Fennoscandian Shield at the actual erosion level shows that the seismic reflection pattern matches the general trends of compositional layering, gneissic banding, and schistosity. The roughly homogeneous structural domains of the crust correspond to relatively large tectonic sheets, 3–5 km thick. Their inner structure commonly is not discernible in reflection patterns. A detailed description of our approach to geological interpretation of reflection seismic images of the crust is given in Mints et al. (2015, Chapter 12).

3.2. Effective acoustic impedance section

The program-and-methodology system of the method of differential seismic (MDS) analysis involves the most effective elements of the controlled directional reception (CDR) procedure and the CMP method. Physical and mathematical aspects of MDS are discussed by Vasiliev and Urupov (1978), Dyadyura (1992) and Stupak (2000). MDS provides an analysis of the kinematic and dynamic parameters of seismic waves. It is based on a reciprocal point technique that provides a solution of the inverse 2D seismic problem for any morphology of reflective boundaries. The data processing begins with the parametric differential representation of seismic records. The main mathematical procedure is velocity sweeping, which means the reflection directional stacking within a small summation window of the order of 5–11 channels of initial records. For each event detected in the stacking procedure a set of parameters is defined: reflection time, time shift (dip), amplitude, frequency, and velocity. Thus, the wave form of the oscillating process is replaced by its parametric description. This reduces the volume of initial information substantially. Each travel-time curve portion represented parametrically is visualized as a vector consisted of ten parameters. Parametric representation is carried out under specified boundary conditions, which are defined by restrictions on the physical properties of the geological medium (for instance, velocity no more than 8000 m/s, frequency within the range of a radiator, a ban on multiples and so on). A set of vectors, which fall into the same base, is written as a standard seismic trace. After seismic record transformation, an interactive editing of seismic data is carried out, rejecting the components which do not bear on the geologic information.

MDS allows the calculation of the effective velocities, location, distribution and dip angles of reflecting elements. At the accepted dimension of depicted events at 400 m, the method made it possible to obtain detailed characteristics of the upper and middle portions of the Earth's crust down to 16–18 km deep. Individual seismic reflections from relatively "smooth" extended surfaces are overlapped and form continuous lines (boundaries). The MDS system also gives an opportunity to analyze travel time and amplitude attributes (parameters) of seismic waves. This, in its turn, makes it possible to proceed the estimation of subsurface petrophysical properties.

Amplitudes of reflected waves (A) are correlated with the acoustic impedance (α) of rock units in contact. The relationship A = f(α) is not defined in quantitative terms, however MDS allows obtaining the distribution of effective acoustic impedance values that characterize the section at a qualitative level (Mints et al., 2015, Chapter 12). Estimations of the effective acoustic impedance are interpolated in a cross-section, then smoothed out to a necessary degree vertically and horizontally and outputted in a colored form onto a section plane. In many cases, effective acoustic impedance sections allow not only the assessment of petrophysical contrasts of contacting rock assemblages, but also the presentation of the structural information in a form more convenient for geological interpretation than seismic reflection patterns, owing to the coherent continuous imaging of a geological medium.

3.3. Principles of magnetotelluric data interpretation

Magnetotelluric (MT) soundings use the observations of the variable electromagnetic field of the Earth to provide information on the electrical conductivity of the crust and upper mantle. The range of this parameter exceeds 12 orders of magnitude from 10^6 Sm/m (for rocks containing minerals characterized by properties of electronic conductors) to 10^{-6} Sm/m and lower (for massive intrusives, permafrost and some other rocks). This enables the physical possibility of detailed resolution of lithotectonic complexes according to the electrical conductivity variability. The restoration of the Earth's deep geoelectric structure on electromagnetic (EM) field observations at the terrestrial surface, the solution of the inverse magnetotelluric problem, is non-unique and usually needs regularization with the help of both adequate mathematical approaches and by a priori constraints. The latter are superimposed according to information on the physical properties of rocks in the region, all available geological information as well as from the data of other, complimentary, geophysical methods (Berdichevsky and Dmitriev, 2008).

For proper interpretation of the observed conductivity anomalies in geological terms it's worth while to take into account, that two mechanisms can contribute to anomalous electrical conductivity of rocks: (i) electronic conductivity caused by occurrence of metallic (sulphide) and graphite-bearing mineral assemblages and (ii) an ionic one, related to the presence of mineralized water in interconnected pore space or to a partial melt. In contrast to geodynamically active regions, where abundant fluids of various composition and origin define the dominance of the ionic mechanism in the bulk conductivity, increase, the relatively cold and dry interiors of Precambrian cratons are mostly characterized by anomalies caused by strong electronic conductors. Only a part of upper crustal anomalously conducting objects are due to meteoric water accumulating in mechanically weakened fault zones.

The geoelectric images of the Precambrian crust contribute significantly to integrated geophysical and geological studies aimed at the reliable reconstruction of the deep-seated lithotectonic features of Precambrian geological units. The important information about internal architecture, and thus of the evolution of the cratons, is obtained due to studies of linearly elongated crustal conductors, which trace Archaean and Proterozoic graphite- and sulphide-bearing volcanic-sedimentary belts both along their surface expression and toward the lower levels of the crust. Such anomalies are known practically in all shields (Zhamaletdinov and Kulik, 2012). The examples of application of the magnetotelluric method to investigations of these tectonic units (boundary mobile belts in other terminology) are presented for basement and shields of the East European (Pajunpää, 1987; Korja et al., 2002; Habibian et al., 2010; Jozwiak, 2012; Vaittinen et al., 2012), African (Weckmann, 2012), and North American (Yin et al., 2014) platforms.

4. The deep crustal sections along the reflection seismic profiles

In this work we involve previously elaborated materials on the crustal structure of the Karelia Craton and Belomorian Tectonic Province with special attention to a marginal domain of the Karelia Craton and its frontier with the Svecofennian Accretionary Orogen (Mints et al., 2009, 2010, 2015, Chapter 12). The profile 4B across the strike of major structural units in the Karelia–Belomorian region is especially informative. It crosses a significant part of the Karelia Craton, its boundary with the Belomorian province, as well as the Palaeoproterozoic East Karelian Belt and some smaller sedimentary-volcanic belts. The 1-EU geotraverse crosses the granite-greenstone complexes of the Khetolamba and Vodlozero microcontinents, partly juxtaposed with tectonic sheets of the Palaeoproterozoic volcanic-plutonic associations and overlain by the Palaeoproterozoic sequence of the Onega Depression. Profiles FIRE-1-2a-2 and FIRE-3-3a cross the Svecofennian Orogen and its boundary with the Karelia Craton (Kukkonen and Lahtinen, 2006) (Figs. 2, 3).

4.1. The Karelia craton, cross-section along the 4B profile

A detailed reflection pattern along the 4B profile (Fig. 4A,C) characterizes the crust and upper mantle from the present-day surface to a depth exceeding 60 km (more than 20 s). Reflection density varies over a wide range. The subhorizontal crust–mantle boundary at 39 km depth is indicated by a sharp reduction in the number and extent of reflections. Towards the eastern end of the profile it dips very gently, reaching a depth of 40 km. On segments where the lower crust is characterized by reducing reflection bin density, the crust–mantle boundary is almost indiscernible. The effective acoustic impedance section from the present-day surface to a depth of 15 km (Fig. 4B) shows a combination of oval and lenticular regions characterized by low acoustic impedance and relatively thin zones with increased and high acoustic impedance. As a rule, zones of increased values conform to clearly expressed wave trains. On the contrary, regions of low acoustic impedance are usually associated with areas of increased transparency, although separate well-expressed wave trains are also contained within such regions. The zone of high acoustic impedance conforms to a zone of extended strong reflections. Near-surface features characterized by increased acoustic impedance are correlated with mapped amphibolite and basalt bodies. Decreased acoustic impedance in turn corresponds to granite, granite-gneiss, and migmatite. We used also the magnetotelluric data obtained in preceding years along a line that is located close to the 4B profile and crosses it at an acute angle (Cherevatova, 2010) (Fig. 4D).

The brightest feature of the crustal section is a distinct variation of both "transparency-reflectivity" pattern and the nature of the structural pattern. Most of the tectonic sheets, varying somewhat in thickness, gradually dip down towards the eastern end of the profile. Strongly reflecting lower crust becomes significantly thinner eastwards, approximately from 20 km to 5 km. A tectonic sheet about 16 km thick at the western end of the profile covers the lower crust. It is approximately 30–35 km thick in the central part of the profile and 10–12 km thick at its eastern end. Associated with this tectonic sheet acoustically transparent oval- and mushroom-shaped regions with low electrical conductivity (Cherevatova, 2010) probably mark the location of large intrusive bodies. Taking into account significant depth, it can be suggested that these intrusions are composed of charnockitic or enderbitic rocks. The base of this sheet-like crustal region lying higher in the section reaches the present-day surface between the 190 km stake and the western end of the profile. Slightly decreasing in thickness, the sheet dips towards the eastern end of the profile, where it occurs at a depth of 26–37 km. On the surface it is represented by the Meso–Neoarchaean uniform leucocratic medium- and coarse-grained TTG gneisses. Gneissosity and banding of migmatites dip southwestwards in conformity with the reflection events' orientation.

A clearly detected inclined sheet that reached the present-day surface between 120 km and 100 km stakes and was marked by a strong reflectivity zone is formed by rocks of increased and high acoustic impedance and increased electrical conductivity. This zone separates the Kovdozero and Khetolamba microcontinents (constituents of the Belomorian Tectonic Province, see Fig. 3) from the Karelia craton and consists of a series of structurally uniform domains of 5–6 km total thickness. In the upper crust, starting at 15 km deep, these domains split, forming a fan

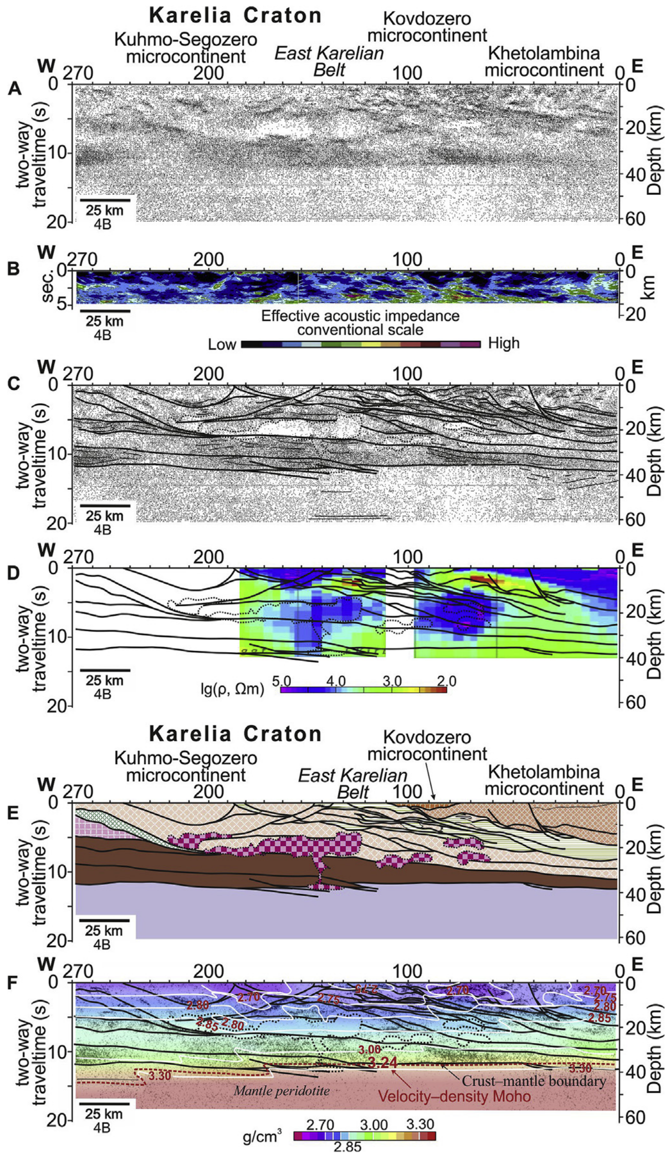

Fig. 4. The Earth's crust and crust–mantle boundary along the 4B profile (modified after Mints et al., 2010, 2015). (A) Migrated CMP section; (B) effective acoustic impedance section; (C) migrated CMP section with deciphered geological boundaries; (D) section with geological boundaries with data on the distribution of the apparent electrical resistivity (based on Cherevatova, 2010); (E) geological model (see Fig. 2 for legend); (F) density section (section of 3D crust model, Glaznev et al., 2015), main tectonic boundaries and certain isodensity contours (white lines), including the velocity–density Moho discontinuity (red dotted line), 3.24 g/cm^3, are shown. Names of the Archaean units appear in Arial normal, names of the Palaeoproterozoic units appear in Arial italics.

consisting of 3–4 individual sheets diverging westwards (Fig. 4E). Mints et al. (2009, 2015) called this tectonic ensemble, formed by alternating tectonic sheets of Neoarchaean TTG gneisses and Palaeoproterozoic sedimentary-volcanic rocks, the East-Karelian imbricate thrust belt. On the profile segment of 80–50 km, asymmetric antiformal folds are clearly observed in the upper part of the crustal section, immediately adjacent to the upper boundary of the tectonic assemblage of the East Karelian imbricate thrust belt. The morphology of the folds indicates on the whole that they formed during thrusting, accompanied by the formation of structural duplexes riding piggy-back in sequence, and the piling-up of displaced tectonic sheets that were deformed into antiformal folds.

The upper part of the crust in the eastern section of the profile (110–0 km) belongs to the Khetolamba microcontinent. Its constituent geological associations are thrust over the East-Karelian imbricate thrust belt. At the same time, the morphology of the folded structures indicates subsequent subsidence of the crust of the Belomorian province, accompanied by the transformation of thrusts into normal faults. The uppermost synformal Kovdozero microcontinent is formed by the granite-greenstone association including greenstone belts, migmatites, and TTG gneisses.

Comparison of the geological model of the deep crustal structure, which is derived from seismic images of the crust (patterns of seismic reflections), and the density model of the crust (Fig. 4F) demonstrates clearly the inconsistency of both models. The discrepancy of the models is especially pronounced in those parts of the section where tectonic plates have a significant slope: near the western and near the eastern edges of the 4B profile.

4.2. *The Karelia craton, cross-section along the 1-EU profile*

The reflection pattern along the 1-EU profile (Fig. 5A) characterizes the crust and upper mantle down to a depth of 70 km (more than 20 s). Reflection density varies over a wide range. The effective acoustic impedance section (Fig. 5B) bears substantial and detailed information on the upper-crust structure and the composition of its constituents.

Along the 1-EU profile, the crust–mantle boundary is clearly seen at 40 km depth in the northern and central parts, and at 50–60 km in the southern segment of the profile (Fig. 5). In contrast to the 4B profile, the crust–mantle boundary is characterized by significant variations both in depth and structure. In the northern segment, 730–830 km, it is represented by a clearly traceable, almost horizontal surface at 40 km deep. This agrees with the 4B profile, which intersects the geotraverse 1-EU near the 700–708 km interval (10–15 km on line 4B respectively). Starting from 850 km, the crust–mantle boundary has serrated outlines distinct in some places and ill-defined in others. The structural shape of the reflection pattern in the lower crust conforming to the serrated form of the crust–mantle boundary indicates subsidence of lower-crustal fragments into the mantle.

A strongly reflecting lower crust can be traced along the major part of the profile. Its smoothly curving top can be traced within the 20–30 km deep interval except for the northern part (700–750 km) where it is at around 35 km. The lower crustal layer, where it is defined, is characterized by the thickness varying from 8–10 km to 30 km. Within the intervals 850–1000 km and 1180–1250 km, the structural pattern indicates bending and dipping of the separate, finely laminated crustal slabs into the mantle, where they reach a depth of 60 km. In some cases, we succeeded in tracing reflections marking the dip of lower crustal slabs into the mantle and their disintegration and "dissolution" within the mantle down to about 70 km deep. Features of the lower crustal boundaries indicate considerable lateral displacements accompanied by deformation of the lower crustal and mantle rocks and subsidence of delaminated fragments of the lower crustal layer. As in the 4B line, the crust–mantle boundary is discontinuous or poorly discernible where the lower crust is characterized by increased transparency.

Within the 700–810 km interval the geotraverse 1-EU crosses the Belomorian Province (see Figs. 2, 3 and 5). The variably reflecting crust above the lower reflectivity zone belongs to the Khetolamba granite-greenstone domain. In contrast to the crust of the Karelia Craton in the 4B section, there are many more reflective domains, but their boundaries are more diffuse. It seems conceivable that the Khetolamba crust is formed by alternating greenstones, gneisses and granite bands and lens-shaped bodies.

The upper crustal structure, part of the East-Karelian imbricated thrust belt, is of special interest in the interval of 800–940 km. The pattern of seismic reflections and the effective acoustic impedance section allow the identification of discrete thin sheets formed by rocks of the Palaeoproterozoic volcano-sedimentary and Neoarchaean granite-gneiss complexes. Interleaving of separate sheets and packages formed by rocks of both complexes indicates their transport southward or southwestward during tectonic displacement.

From the 940 km stake up to stake 1250 km (see Figs. 2, 3 and 5), the geotraverse crosses the granite-greenstone complex of the Vodlozero microcontinent, partly juxtaposed with tectonic sheets of the Palaeoproterozoic volcanic-plutonic associations and overlain by the Palaeoproterozoic sequence of the Onega Depression. A distinctly outlined zone of intense reflections, composed of rocks with increased acoustic impedance, is seen in the middle of this sheet. This zone is traced with certain complications for ~300 km in the interval 975–1250 km and is confidently correlated with greenstone belts, which extend in the near-meridional direction along the western boundary of the Onega Depression. From 960 km to 1120 km, the geotraverse crosses the Palaeoproterozoic Onega Depression mainly along its northwestern and western margins. The section distinctly depicts the rock complex that fills the Onega Basin. Its bottom reaches 5–6 km in depth toward the centre of the depression. The crust immediately underlying the volcanic-sedimentary complex is subdivided into lenticular blocks, which emerge toward the northern end of the profile. Finally, the southern end of the profile, approximately from 1190 km, crosses volcanic-sedimentary sequences of the Svecofennian Accretionary Orogen plunging as a homocline to the south and cut through by rapakivi granite, which is characterized by low acoustic impedance.

The crust–mantle boundary is disturbed or poorly discernible at the profile segments where the lower crust is acoustically transparent. The largest fragment of the crust of this type, in interval of 1070–1200 km, is located above the lower-crustal zones plunging into the mantle towards each other. The crust in this interval is homogeneous in terms of acoustic transparency and exhibits low intensity and vague orientation of reflections. The upper boundary of the homogenized segment of the crust, which has replaced and amalgamated the sheets of the lower and middle crust, is located at a depth of 15–20 km, while the lower boundary is traced indistinctly at a depth of ~55 km. The underlying upper mantle is characterized by nonuniformly distributed and occasionally rather intense reflections. In general, the seismic image of the crust and the adjacent mantle in this interval is uniform and homogeneous without sharp gradients of acoustic impedance and sharp changes of rock compositions. As along profile 4B, a strongly reflecting lower crust can be traced along the greater part of the profile, excluding 1070–1200 km segment. The thickness of the lower-crustal layer is around 20 km thick and exceeds this value at the southern end of the profile within the 1200–1300 km interval (Fig. 5). The mantle directly underlying the serrated crust–mantle boundary is distinguished by the presence of irregularly distributed, partly rather strong reflections. In a sense, this zone may be interpreted as a crust–mantle mixture. Alternatively, this zone may consist of mafic eclogite facies rocks of crustal affinity.

4.3. The Svecofennian Accretionary Orogen, FIRE project

The patterns of seismic reflectors that produce seismic images of the crust and crust–mantle boundary of the Svecofennian accretionary complex in the profiles FIRE-1-2a-2 and FIRE-3-3a, are in general of a similar type (Figs. 2, 6 and 7). The consecutively plunging packets of reflectors are related to the rocks of the Svecofennian accretionary complex. The packets plunge at angles of 10°–12° towards the eastern ends of both profiles, and diffusive crust–mantle boundary constrains the packets from below. For the eastern segments of both profiles, where the reflectors are controlled by the structure of the border zone between the Karelia Craton and the Svecofennian Accretionary Orogen, an opposite dip of the reflectors is typical (Mints et al., 1995). The tectonic sheets, 10–20 km thick each, are traced from the surface, where their position and boundary configuration are defined by the geological map, to the crust–mantle boundary at a depth of 60 km approximately. These sheets are mainly composed of rocks formed in island-arc and inter-arc basin settings. The seismic images of tectonic sheets are periodically interrupted by acoustically transparent segments apparently related to accommodation of intrusive bodies; however, the absence of reliable correlation of these segments with corresponding objects at the surface does not allow us to identify them at depth with full confidence.

A special position in the accretionary orogen structure belongs to CFGC, which is one of the largest granitoid massifs of Fennoscandia. In the section along profile FIRE-2-2a-1, it is clearly seen that the massif or a significant part thereof is represented by a gently dipping sill-like body composed of a layered complex of rocks with the maximum thickness not exceeding 10–12 km. Our opinion is in agreement with the interpretation presented earlier by Finnish colleagues (Kontinen and Paavola, 2006; Korja et al., 2006a). The near horizontal intrusive body cuts off a series of slantwise plunging sheets. The section along the FIRE-3-3a profile demonstrates clearly that the eastern part of the granitoid massif is a constituent of the accretionary complex. In conformity with the structure of the accretionary complex as a whole, this branch of the massif plunges to the east and is traced from surface to the crust–mantle boundary (Mints et al., 2018).

The crust–mantle boundary underlying the Svecofennian

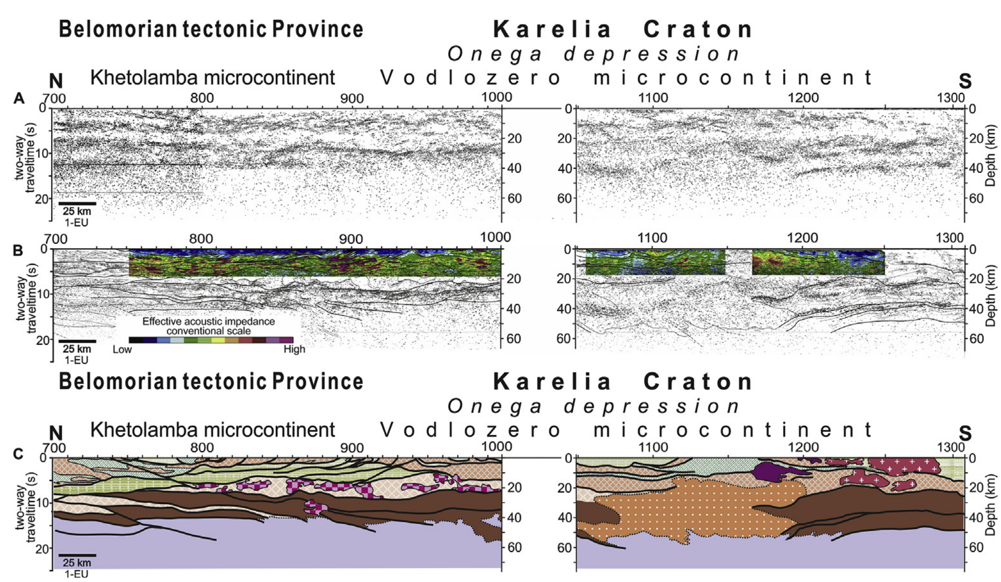

Fig. 5. The Earth's crust and crust–mantle boundary along the 1-EU profile (modified after Mints et al., 2010, 2015). (A) Migrated CMP section; (B) migrated CMP section with deciphered geological boundaries and effective acoustic impedance section for upper crust; (C) geological model (see Fig. 2 for legend). Names of the Archaean units appear in Arial normal, names of the Palaeoproterozoic units appear in Arial italics.

Accretionary Orogen has an indented outline and diffuses appearance along the entire extent of profiles FIRE-2-2a-1 and FIRE-3-3a: the sheets of accretionary complex consecutively reach the crust–mantle boundary as if dissolving in the acoustically transparent mantle body (Figs. 6, 7). The model density calculations for the lower crust and the upper mantle in the Svecofennian Orogen do not display any significant jump in transition from the lower crust to the upper mantle (Glaznev et al., 2015). A similar estimate of density was earlier obtained by Kuusisto et al. (2006). A maximum penetration depth of tectonic sheets into the mantle recorded in seismic sections reaches 75 km; the domain of maximal values is related to the Karelia Craton and Svecofennian Orogen boundary.

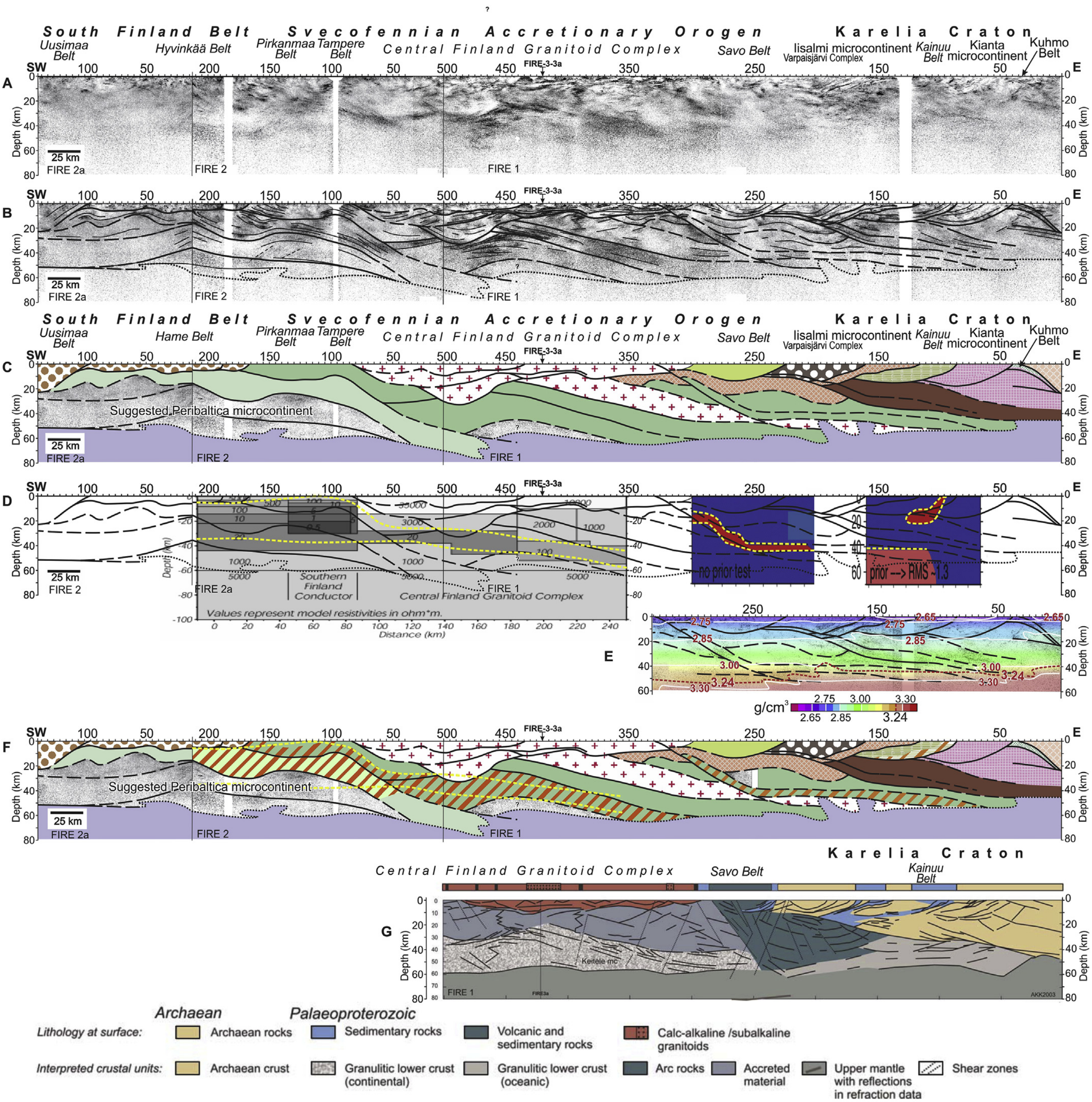

Fig. 6. The Earth's crust and crust–mantle boundary along FIRE-2a-2-1 profile (modified after Mints et al., 1998). (A) Migrated CMP section after (Kukkonen and Lahtinen, 2006); (B) migrated CMP section with deciphered geological boundaries; (C) seismogeological model (see Fig. 2 for legend); (D) seismogeological model with data on the distribution of the apparent electrical resistivity: on the left, the results of MT soundings in the southern part of the SVEKA profile are shown (MTS profile practically coincids with the seismic profile, the electrical resistivity values are given in Ohm · m (after Korja et al., 2002)), in the centre and in the eastern part of the profile, electrical resistivity models are projected from nearby profiles (red color shows conductors) (after Vaittinen et al., 2012); (E) density section (section of 3D crust model (Glaznev et al., 2015)), main tectonic boundaries and certain isodensity contours (white lines), including the velocity–density Moho discontinuity, 3.24 g/cm^3; (F) geological section with zones of increased electrical conductivity; (G) seismogeological model with its own legend (after Lahtinen et al., 2009). Names of the Archaean units appear in Arial normal, names of the Palaeoproterozoic units appear in Arial italics.

4.4. The Svecofennian Accretionary Orogen, results of magnetotelluric sounding

In preceding years, significant magnetotelluric data were obtained by Finnish and Russian researchers in the studied part of the Svecofennian Accretionary Orogen. These data allow us to expand our knowledge on the composition of rocks making up structural crustal domains recognized in seismic sections. We have analyzed published geoelectric cross-

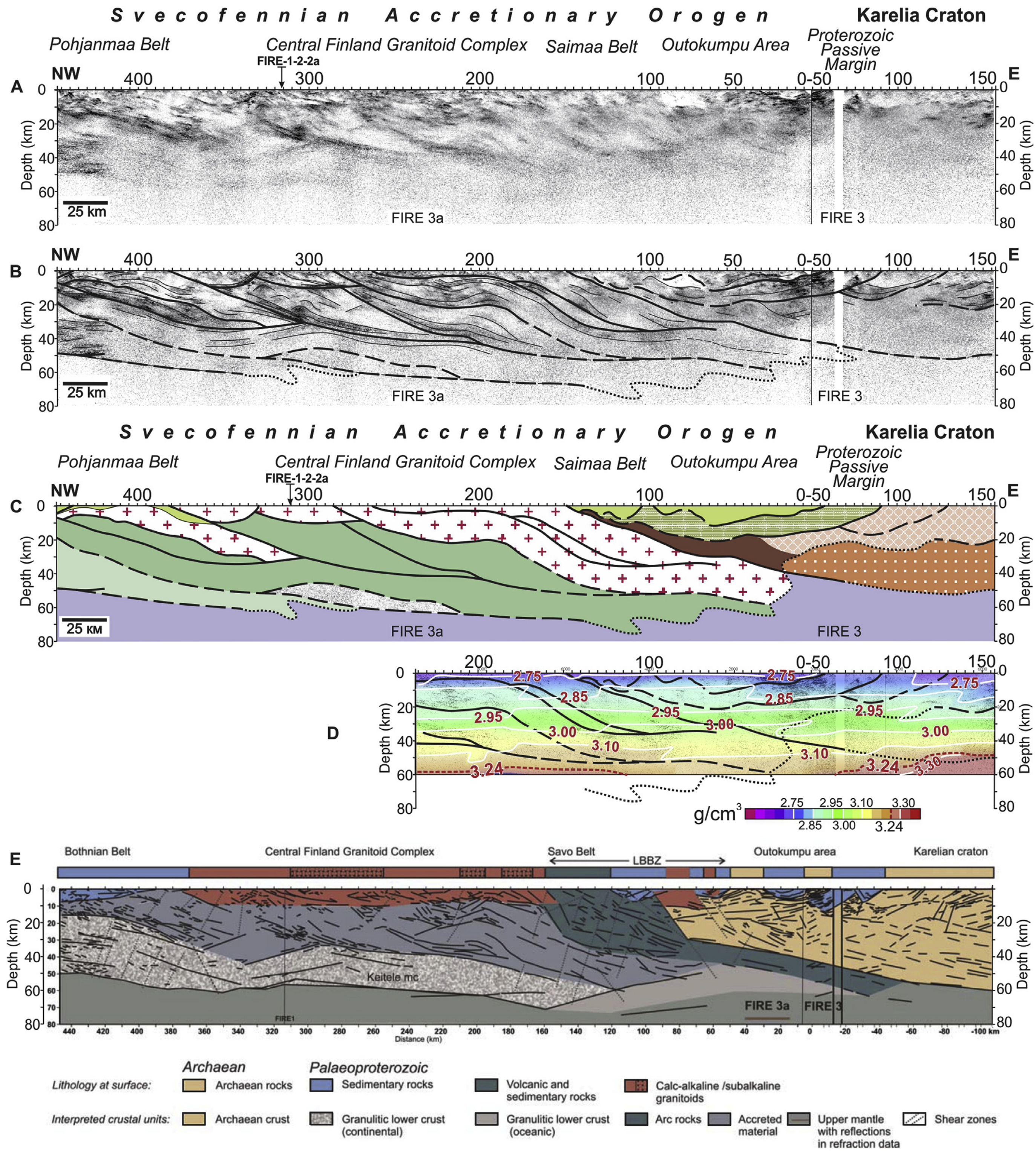

Fig. 7. The Earth's crust and crust–mantle boundary along FIRE-3a-3 profile (modified after Mints et al., 1998). (A) Migrated CMP section (after Kukkonen and Lahtinen, 2006); (B) migrated CMP section with deciphered geological boundaries; (C) seismogeological model (see Fig. 2 for legend); (D) density section (section of 3D crust model; Glaznev et al., 2015), main tectonic boundaries and certain isodensity contours (white lines), including the velocity–density Moho discontinuity, 3.24 g/cm^3; (E) seismogeological model with its own legend (after Lahtinen et al., 2009). Names of the Archaean units appear in Arial normal, names of the Palaeoproterozoic units appear in Arial italics.

sections along the magnetotelluric sounding profiles, which intersect the orogen in immediate proximity to profile FIRE-2-2a-1 (Korja et al., 2002; Vaittinen et al., 2012). The comparison of these data with results of geophysical surveys, boreholes and field observations showed that increased regional electrical conductivity is mostly related to rocks with significant amounts of graphite and frequently with admixture of sulphides. The cryptocrystalline and/or incompletely crystalline graphite occurs in sedimentary rocks affected by low- and moderate-grade metamorphism; the coarse- and medium-flaked graphite is characteristic of granulites. Two-types of anomalies of electric conductivity are recognized: (1) in rocks of passive margin of the Karelia Craton and in rocks of the Svecofennian accretionary complex, where anomalies are related to the cryptocrystalline and/or incompletely crystalline graphite and (2) in the South Finland paragranulites containing coarse- and medium-flaked graphite. In turn, we can fill the "structural skeleton" of the crust, inferred from seismic sections, with the information on electrical conductivity of rocks making up these structures, and consequently we are able to distinguish tectonic sheets consisting of volcanic and sedimentary rocks from the sheets formed by granitoids more reliably (Fig. 6). Furthermore, anomalies of electric conductivity make it possible to recognize the graphite-bearing sedimentary rocks of blind (not approaching the surface) sheets of the accretionary complex in the section along the profile FIRE-2-2a-1.

At the base of the Karelia Craton and of the granulite-gneiss South Finland Belt, the image of the crust–mantle boundary partly retains a diffuse character, but acquires a flat horizontal outline. Representative cross-sections along the 4B profile (Fig. 4) and 1-EU geotraverse (Fig. 5) have demonstrated that the Karelia Craton is underlain almost completely by the lower crustal reflectivity zone, corresponding to Palaeoproterozoic mantle-plume mafic underplating (Mints et al., 2010, 2015). A weak expression of reflectivity zone at the base of the Karelia Craton along profiles FIRE-2-2a-1 and FIRE-3-3a is caused by thinning of the crust of the Karelia Craton during the formation of the passive margin.

4.5. *Velocity-density Moho discontinuity and crust–mantle boundary*

The sections of the 3D density model of the crust in the studied area (Glaznev, 2003; Glaznev et al., 2015) along 4B (Fig. 4F), FIRE-2-2a-1 (Fig. 6E) and FIRE-3-3a (Fig. 7D) profiles are in agreement with general trends that demonstrate subhorizontal density layering locally with smooth bending. The sections also show systematic increase in density with depth along with smoothing of lateral density variations, while the main structural features of the medium are maintained. As follows from comparison of density and geological sections, the morphology of the density image depends only insignificantly on geological structure of the crust.

In the 4B profile (Fig. 4), where the crustal base is clearly traced as the lower crustal layer (reflectivity zone), an abrupt increase in density to mantle values (3.24–3.30 g/cm^3) is noted at the bottom of this level at a depth of 40 km; the crust–mantle boundary and Moho discontinuity are coordinated and have flat outlines. In the interval of 160–270 km along the profile, where the mantle is enriched in reflecting elements immediately adjacent to the crust, isodensity contours of 3.00 and 3.24 g/cm^3 plunge from a depth of 38 km to 40–45 km. The increase of the Moho discontinuity depth in the western segment of the profile is apparently caused by its approaching the Svecofennian Orogen.

In the geological section along FIRE-2-2a-1 (Fig. 6), the diffuse crust–mantle boundary has complex indented outlines controlled by consecutive plunging of tectonic elements pertaining to the accretionary complex into the mantle and disappearance of their seismic image in the mantle. The velocity–density Moho discontinuity corresponding to the isodensity contour of 3.24 g/cm^3 is characterized by a flat shape complicated by a series of stepwise bends. The localization of the most distinctly curved isodensity contour is directly related to subsidence of the sheets pertaining to the accretionary complex into the mantle. In the south-western segment of the FIRE-2-2a-1 profile within the interval of 215–335 km, where the seismic CMP image of these sheets gives evidence of their penetration below the 50 km deep, the isodensity contours of 3.24 and 3.30 g/cm^3 also reach a depth of about 50 km. A similar pattern is observed along the FIRE-3-3a profile (Fig. 7), where the following relationships are observed: Moho discontinuity marked by the isodensity contour of 3.24 g/cm^3 plunges to a depth of about 70 km within the intervals where the plunging tectonic sheets also reach a maximum depth; the isodensity contour of 3.24 g/cm^3 ascends by 15–20 km beneath the Karelian Craton.

5. Discussion

The detailed 3D representation of the deep crustal structure of the Svecofennian Accretionary Orogen and the adjacent tectonic units – Karelia Craton and South Finland granulite-gneiss belt (Figs. 1, 3 and 8) – makes it possible to combine and to link together the geological map (Fig. 2) and deep sections of the crust (Figs. 4–7). The juxtaposition of seismic crustal images and data on the distribution of the electronically conductive graphite-bearing metasedimentary rocks intercalating with volcanic layers and granite bodies characterized by a high electric resistivity, made it possible to trace the tectonic sheets of accretionary complex from the surface down to the crust–mantle boundary with much more confidence.

The 3D model of the Early Precambrian crust substantially changes previous concepts about the crust of the eastern Fennoscandian Shield as a combination of blocks with subvertical margins and individual internal layering. Obviously, the positions of the gently dipping boundaries on the present-day surface are determined by the erosion level and, as a result, these boundaries cannot be recognized as subvertical boundaries of the tectonic blocks in the traditional sense.

5.1. *Deep crustal structure of the Karelia Craton*

The Archaean granite-greenstone crust of the Kuhmo-Segozero microcontinent is a wedge-shaped body that reaches ~30 km in thickness near the western and southwestern margins of the microcontinent and gradually becomes thinner with plunge to the east beneath the Khetolamba and Vodlozero microcontinents. In the section along the 1-EU geotraverse, the southeastern margin of the Kuhmo-Segozero microcontinent occupies a middle level of the crust (Mints et al., 2010, 2015). The section along cross-traverse 4B indicates that the tectonic sheet formed by the Kuhmo-Segozero microcontinent was displaced and inclined after formation of isometric, acoustically transparent bodies interpreted as large plutons presumably of an enderbite-charnockite composition. The Kovdozero microcontinent is represented in section along cross-traverse 4B as a synformal tectonic sheet that overlies the Archaean granite-greenstone complex of the Khetolamba microcontinent.

The northeastern boundary zone of the Karelia craton and the Lapland sector of the Palaeoproterozoic intracontinental orogen (Mints et al., 2009, 2015; Mints, 2011) are represented by the East Karelian imbricate thrust belt. This belt is an alternation of tectonic sheets composed of Archaean granite-greenstone and Palaeoproterozoic volcanic-sedimentary assemblages. The detachment surface at the base of this belt is traced at a depth of 10–15 km and then plunges to a depth of 27 km at the intersection of the 1-EU geotraverse and of cross-traverse 4B. The 1-EU geotraverse at a distance between 950 km and 1150 km crosses the western peripheral area of the Palaeoproterozoic Onega Depression. In the section along the 1-EU line, the thickness of the volcanic-sedimentary complex filling this depression reaches 5–6 km. In the middle part of the crust, a domain exists, where magmatic bodies most probably consisting of enderbite and charnockite are localized as a result of partial melting of the crust and fractionation of the melt.

The main features of *the Palaeoproterozoic mafic lower crustal layer* in combination with structural relationships between this complex and

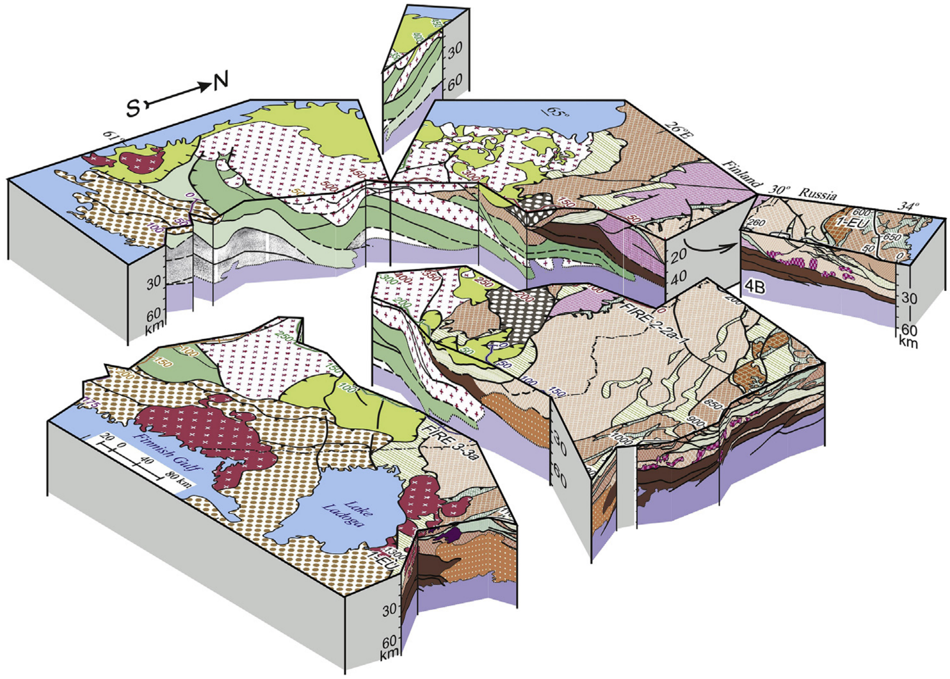

Fig. 8. 3D model (block diagram) of the deep crustal structure of the Svecofennian Accretionary Orogen and adjacent tectonic units: the Karelian craton and the Southern Finland granulite-gneiss belt (reworked after Mints et al., 1995). See Fig. 2 for legend.

granite-greenstone crust suggest that the lower crustal layer was formed at the end of the Palaeoproterozoic due to the ascent of a mantle plume (see Mints et al., 2015, Chapters 8 and 17 for more details). The thickness of the lower crust reaches 25–30 km as a result of stacking in the boundary zone with the Svecofennian orogen (Figs. 4 and 8). With distance from this zone inward to the Karelian continent and further to the east, the thickness of the lower crust decreases down to 8–10 km near the boundary with the Khetolamba microcontinent. The lower crustal layer of the Karelian-Belomorian region is only locally interrupted by acoustically transparent bodies.

Thus, in the process of the Palaeoproterozoic evolution, the crust of the Karelian-Belomorian region acquired a three-level structure.

(i) The upper level is the alternation of tectonic sheets composed of Archaean granite-greenstone and granulite-gneiss complexes with sheets formed by the Palaeoproterozoic volcanic-sedimentary assemblages.
(ii) The mid-crustal level is formed predominantly by the Archaean granite-greenstone complexes, which contain oval and mushroom-like bodies intruded during the Palaeoproterozoic.
(iii) The lower crust formed by the Palaeoproterozoic underplating of mantle magmas. The seismic image of this crust corresponds to the reflectivity zone. The lower crust consists of Archaean and Palaeoproterozoic mafic intrusive rocks and gabbroanorthosites metamorphosed in the Palaeoproterozoic under granulite facies conditions.
(iv) The boundaries between Archaean microcontinents are modified to a varying degree by the Palaeoproterozoic processes. In some cases, the frontier zones are formed with the participation of the Palaeoproterozoic volcanic-sedimentary assemblages.

5.2. Deep crustal structure and evolution of the Svecofennian Accretionary Orogen

The internally coordinated 3D model of deep crustal structure and crust–mantle boundary of the Svecofennian Accretionary Orogen makes possible its application for reconstruction of the geodynamic evolution of the orogen as well as for finding ways of modeling the Palaeoproterozoic evolution of Lauroscandia as a whole (Mints, 2007, 2013; Mints and Eriksson, 2016). The combination of two seismogeological sections establishes the predominant northeastern plunging of rocks pertaining to the accretionary complex. The plunging of tectonic sheets was accompanied by right-lateral strike-slip displacements in both the Karelia Craton and the Svecofennian accretionary complex. The frontier domain is characterized by development of crocodile-type structure, delamination, and mutual wedging of the crust typical of collisional orogens. The accretionary complex is restricted below by diffuse crust–mantle boundary which is indented in outline. The deep-seated edges of plunging tectonic sheets are visually dissolved in the mantle.

5.3. Density heterogeneity and nature of density layering of the crust

According to velocity-density models, the regional structure of the crust is determined largely by nearly horizontal boundaries, which reflect gradual variation of rock densities with depth. The crustal layers bounded by isodensity surfaces are, as a rule, discordant with respect to the inclined boundaries of geological complexes in seismic images of the crust (Figs. 4, 6 and 7). As was noted above, density heterogeneities (crustal layers) reveal only local and incomplete interrelations with localization and morphology of geological bodies.

The isodensity contours in crustal sections are largely oriented in a subhorizontal direction and approximately parallel to the present-day topography, and this is also valid for other Archaean terrestrial cratons (Abbott et al., 2013). It is evident that only regional lithostatic pressure remains the crucial factor of variations in density of rocks at the middle and lower crustal levels, where metamorphism is blocked by low temperature (~400 °C in the lower crust and no higher than 300 °C in the middle crust). Despite density changes under the lithostatic pressure, however, the structure of the medium formed earlier in the course of sedimentation, magmatic activity, metamorphism, and tectonic reworking remained intact. Heterogeneity of crustal and mantle heat flows (Glaznev, 2003; Glaznev et al., 2004); zones of stress relaxation (Lyakhovsky and Ben-Zion, 2009); tectonic stresses as a result of interaction of density heterogeneities (Glaznev et al., 1991; Rebetsky, 2007) are local factors. The increase in density with depth is accompanied by appreciable decrease in density differentiation between rocks of various compositions.

For a long time, it was suggested that increase in density of continental crust with depth is determined by variation in composition of rocks as the main factor. The clearest expression of these ideas was the assumption that “granitic” and “basaltic” geophysical layers are separated by Conrad surfaces in the crust (Conrad, 1925). Despite the conditionality of these terms always being emphasized afterward, the idea of density layering of the continental crust with direct change of its bulk composition has retained its appeal (Christensen and Mooney, 1995). In the opinion of Kuusisto et al. (2006), the available information on the crust in the predominant part of the Fennoscandian Shield (including the area discussed in this paper) shows that layers with different velocities participate in crustal complexes. According to these authors, the contribution of mafic rocks increases with depth. The upper crust consists primarily of gneisses in combination with granite and granodiorite. Amphibolite and quartzite are subordinate in abundance; the role of amphibolite increases in the middle crust.

In our opinion, the structure of the accretionary complex of the Svecofennian Orogen, composed of tectonic sheets, which plunge beneath the margin of the Karelian Craton and underlie Archaean rocks of this craton for a significant distance, can hardly be represented in terms of this model. On the contrary, it can be stated that the quantitative proportion of different rocks in plunging tectonic sheets do not undergo any systematic variations, neither in each particular sheet, nor in the accretionary ensemble as a whole.

The nature of rock compaction under lithostatic pressure, the most important factor to determinate the state of continental crust, was not so far studied sufficiently. Taking into account that compaction of ancient rocks is controlled by the recent state of the crust or close to such a state, metamorphism, often mentioned as a substantial factor of compaction, should be excluded from possible reasons, at least for the upper and middle crust. The closure of fractures and pores with release of solutions and fluids contained therein is undoubtedly an important factor, however, alone it is not able to provide the observed compaction of rocks significantly exceeding the results of laboratory experiments on rock samples under high pressure (for example, from 2.80–2.85 g/cm^3 to 3.0–3.1 g/cm^3 in the case of sedimentary and volcanic rocks of the Svecofennian accretionary complex). It should be also kept in mind that variation in density of rocks is reversible, because boundaries of crustal layers which are variable in density, except for the uppermost ones, are not cut off by erosional topography, and the pattern of density layering is similar for young orogens at the stage of growth and intense denudation and for equilibrated isostatic platform regions.

The rheology data predict that at a constant strain rate, deformed rock may stay elastic only if the applied stress is below certain strength, called the yield stress. At this stress it will undergo either brittle or ductile deformation. Ductile strength depends on temperature; brittle strength depends on pressure. Constitutive laws used to obtain yield-stress envelopes are extrapolated from data of experimental rock mechanics. These laws are subject to large uncertainties because (1) the lithospheric conditions are only partly reproducible in the experiments and (2) the results are extrapolated from laboratory time and space scales to geological scales (Burov and Diament, 1996). The data presented in our article indicate the probability of the elastic behavior of the continental crust at geological time and space scales. A challenge for the geophysics and rock physics communities is elucidation of specifics and mechanisms of the global compaction of the continental crust.

5.4. *The nature of the lower crust, crust–mantle boundary, and velocity–density Moho discontinuity beneath the Karelian Craton and the Svecofennian Accretionary Orogen*

It has been reliably established that the Precambrian crust of the Fennoscandian Shield, similar to all other continental domains, is characterized by subhorizontal density layering: the high-velocity and high-density lower crust, variable in thickness and depth, occurs at the base of the Svecofennian Orogen and the adjacent tectonic subdivisions of regional rank as well (Korsman et al., 1999; Bock et al., 2001; Bogdanova et al., 2006; Janik, 2010; Janutyte et al., 2014; Glaznev et al., 2015). This circumstance suggests that interpretation of composition and origin of the lower crust at the base of the Svecofennian Orogen should be comparable with similar characteristics at the base of neighboring domains (Figs. 4F, 6E and 7D).

Another source of information is provided by seismic images of the crust (patterns of seismic reflections) described above. The deep crustal structures of the Svecofennian Accretionary Orogen and the Karelia Craton possess a series of principal distinctions (Mints et al., 2010, 2015, Chapter 12; Glaznev et al., 2015), which are systematically listed in Table 1 below.

In the seismic CMP sections, the lower crust is commonly identified with reflectivity zone localized immediately above the crust–mantle boundary, in other words, with a zone of intense seismic reflections, which fill this zone completely or to a significant degree, depicting an image of the layered lower crust (Mooney and Meissner, 1992). Such a reflectivity zone (lower crustal layer) 7–12 km thick continuously underlies the Archaean crust in the eastern Fennoscandian Shield, including the Karelian, Kola cratons, and Belomorian Province (Mints et al., 2009, 2010, 2015; Mints, 2011).

In the region considered in this paper, the lower crust of this type is observed in section along the 4B profile (Fig. 4). The pattern of seismic

Table 1
The main features of the seismic images of the crust of the Karelia Craton and Svecofennian Accretionary Orogen.

No.	Karelia Craton (profile 4B, geotraverse 1-EU)	Svecofennian Orogen (profiles FIRE-1-2a-2 and FIRE-3-3a)
1	The upper to middle crust of granite-greenstone type is characterized by gentle dipping tectonic layering. Inclined tectonic boundaries are confined to relatively narrow zones dividing large structurally homogeneous domains.	The crust of accretionary complex is characterized by eastward inclined tectonic layering and consecutive plunging of tectonic sheets. Tectonic sheets about 15 km thick are composed of volcanic and sedimentary rocks, including electronically conductive graphite-bearing sediments and granitoids of high electrical resistivity.
2	Structure of the upper crust expressed in pattern of seismic reflections is readily correlated with geological map.	The seismic image of sill-like CFGC displays structural and likely compositional delamination, which was not observed at surface.
3	The middle crust is distinctly recognized as an acoustically translucent domain, about 10–15 km thick. Transparent bodies in areas with increased thickness can be compared with granitoid plutons by a series of attributes.	The middle crust does not have a special expression in the seismic reflection pattern.
4	The granite-greenstone crust is overall underlain by reflectivity zone, which is composed of granulitic basic rocks formed as a result of underplating with hot magma of mantle-plume nature. The structure of this complex points to lateral displacements in form of intracrustal thrusting and wedging.	Reaching a lower crustal level, the inclined tectonic sheets of accretionary complex lose distinct outlines and are replaced by the homogeneous acoustically translucent medium, where the boundaries dividing separate sheets are traced only in fragmentary fashion, or are simply inferred.
5	The crust–mantle boundary (lower boundary of reflectivity zone), with few exceptions, is smooth, sharp, horizontal or subhorizontal. In particular areas the boundary is interrupted as a result of curving and plunging of lower crustal tectonic sheets into the mantle. These sheets are as if dissolved in acoustically transparent mantle.	The crust–mantle boundary does have diffusive character. Crust–mantle transition is recorded in gradual disappearance of vaguely pictured boundaries of tectonic sheets and gradual transition of acoustically homogeneous and translucent lower crust to transparent mantle.

reflections demonstrates an almost horizontal smooth crust–mantle boundary lying at a depth of 37–39 km. Along most of the 4B profile, the crust–mantle boundary practically coincides with the velocity–density Moho discontinuity, which is comparable to an isodensity contour (surface) of 3.24 g/cm^3 in value. According to Glaznev et al. (2015), in the central part of the Karelian Craton, the Moho discontinuity depth varies from 38 km to 45 km. More significant depths as compared with the 4B profile are characteristic of the Kianta and Iisalmi terranes in the western part of the craton, where they reach 42–45 km. It should be noted that the depth of the Moho in this region is 46–52 km according to Tesauro et al. (2008) and Grad et al. (2009), and 48–52 km according to Kozlovskaya et al. (2004). Even greater Moho depth is suggested by Silvennoinen et al. (2014). The lower crustal layer (reflectivity zone), 5–15 km thick, is overall bounded by crust–mantle boundary of this type (Mints et al., 2009; Mints, 2011). The increase in thickness of the lower crustal layer is related to hummocking (over- and underthrusting) of tectonic sheets at the bottom of the crust. In particular, significantly increased thickness of the lower crustal layer of up to 20 km is noted at the western and southwestern margins of the Karelian Craton along its boundary with the Svecofennian Orogen (Figs. 4, 5 and 8). In this region, the lower crustal layer is not only characterized by elevated thickness but is also raised due to the mutual over- and underthrusting of the rock complexes pertaining to the Karelian Craton and the Svecofennian Orogen. This implies that the lower crustal layer of the Karelian Craton was formed before Late Palaeoproterozoic collisional events.

The lower crustal layer and underlying upper mantle at the boundary zone between the Kola Craton and Belomorian Province are cut through by Devonian kimberlite and lamproite pipes and dikes, which are exposed at the coast and on islands of Kandalaksha Bay of the White Sea and which contain lower crustal xenoliths mainly composed of garnet granulite identical to mafic granulites and metagabbro-anorthosites of the Lapland and Kolvitsa–Umba granulite-gneiss belts. In the present-day structure, these rocks belong to the lower crust and occur at a depth of ~45 km (Mints et al., 2009, 2010, 2015). Age of zircons from the garnet granulite covers a range of 2.84–0.26 Ga, which combines four discrete time intervals: Neoarchaean (2.84–2.74 Ga), Palaeoproterozoic (2.47–2.41 Ga and 1.83–1.75 Ga), and Palaeozoic (0.33–0.26 Ga) (Downes et al., 2002; Vetrin, 2006; Vetrin et al., 2009, 2018). These dates correspond to the main events in the long history of formation and transformation of the crust. The ages of Early Palaeoproterozoic zircons coincide with ages of the known manifestations of magmatism and high-temperature metamorphism of granulite and eclogite facies (Mints et al., 2007, 2010), which began Palaeoproterozoic evolution initiated by mantle plumes responsible for formation of the lower crustal granulite–mafic layer. A model of the layered lower crust, which is formed under extension accompanied by sheet-like intrusions of mafic mantle-derived magma, was considered by Holliger and Levander (1994). Similar conclusions concerning the origin of the lower crustal reflectivity zone were drawn by McBride et al. (2004) and Meissner et al. (2006). Thus, we have sufficient grounds to infer that the lower crust, which underlies the Archaean Karelian Craton as a reflectivity zone bounded by smooth nearly horizontal crust–mantle boundary combined with velocity–density Moho discontinuity of the first type, was formed in the Palaeoproterozoic as a result of tectonothermal and magmatic processes of plume type. Correspondingly, the Archaean lithospheric mantle of the Karelian Craton was transformed under the influence of Palaeoproterozoic plumes (Mints et al., 2010, 2015).

The crust of the western Karelian Craton in the Iisalmi terrane immediately bordering on the Svecofennian Orogen is also characterized by deep xenoliths carried up by Late Neoproterozoic kimberlite magmas in the Kaavi–Kuopio area located between FIRE-2-2a-1 and FIRE-3-3a seismic lines (Fig. 2). As can be seen from seismic cross-section along the FIRE-2-2a-1 profile, the base of the Iisalmi terrane is located at a depth of no more than 20 km (Fig. 6). In the Kaavi–Kuopio area, the Archaean crust is underlain by a thick (>40 km) packet of tectonic sheets related to the Svecofennian accretionary complex, which plunges eastward beneath the Karelian Craton. The high-density (up to 3.0–3.24 g/cm^3) rocks at the base of the crust are comparable to the Palaeoproterozoic rocks of this complex. The confirmation of this inference can be obtained by comparing the geological map (Fig. 2) with geological sections along the FIRE-2-2a-1 and FIRE-3-3a seismic profiles (Figs. 6, 7). Deep xenoliths are mainly composed of Archaean and Palaeoproterozoic mafic granulites; the age of their protoliths reaches 3.7–3.5 Ga (Peltonen et al., 2006). Summing up geochronological data on granulites from xenoliths and the Varpaisjärvi Complex exposed nearby (Hölttä et al., 2000a), the age of Archaean granulite facies metamorphism can be determined at 2.7–2.6 Ga. The peak parameters of granulite facies metamorphism estimated from the data on xenoliths correspond to 800–930 °C and 8.4–12.5 kbar (30–45 km) (Hölttä et al., 2000b). The peak parameters for the Varpaisjärvi Complex are 800–900 °C and 9–11 kbar (32–39 km) (Hölttä and Paavola, 2000). Evidence for superposition of Palaeoproterozoic granulite facies metamorphism on the Archaean rocks of the Varpaisjärvi Complex in the time interval of 2.5–1.7 Ga was obtained only for xenoliths and was not supported by rocks from the Varpaisjärvi Complex (Hölttä et al., 2000a; Peltonen et al., 2006). In addition, zircons younger 1.85 Ga that crystallized under a thermal impact following the Svecofennian Orogeny were found in xenoliths. It is evident that xenoliths of granulites from the Kaavi–Kuopio pipes and the Varpaisjärvi granulites belong to the same rock complex, which occurs now at a relatively high level in the crust and at a significant distance from the crust–mantle boundary. Most likely, these xenoliths should be regarded as relics of the Neoarchaean lower crust rather than fragments of the recent lower crust, as was suggested by Kuusisto et al. (2006) and Peltonen et al. (2006).

The pattern of seismic reflections characterizing the Late Palaeoproterozoic accretionary complex of the Svecofennian Orogen is separated from the mantle by a wide translucent domain. Assuming a density of 3.0–3.24 g/cm^3, this domain is regarded as the lower crust, which is separated above from the ensemble of inclined tectonic sheets, and below by the diffuse transitional zone with serrate outlines from the mantle. The velocity–density Moho discontinuity follows morphology of the crust–mantle boundary in general outlines and a smoothed form. The well-known Moho depression corresponds to the area of subsidence of the Svecofennian accretionary complex in the boundary zone with the Karelian Craton and further beneath its margin. In this area, the accretionary complex is made up of two packets of tectonic sheets plunging to the east and divided by the SE-trending transform strike-slip fault. The width of the northern packet is 250 km; the width of the southern packet exceeds 100 km. The depth of the velocity–density Moho discontinuity in the region of plunging of both packets varies from 45 km to 60 km. The contours of plunging tectonic assemblies advance far to the east relative to the boundary between Svecofennian Orogen and Karelian Craton in compliance with the concept assuming subduction of island-arc, back-arc, and inter-arc basins of the Svecofennian Orogen beneath the margin of the Karelian Craton. As concerns evidence for Svecofennian subduction, both refraction and reflection seismic profiling yielded the same results. Structural features of the Svecofennian Orogen, arising at the stage of accretion, are not overlapped and obscured by transformations, which might have been responsible for subhorizontal velocity and density layering of crust revealed by deep seismic sounding and gravity and density simulation.

Thus, structural characteristics of geological crust–mantle boundary and velocity–density Moho discontinuities at the base of the Archaean Karelian Craton and the Palaeoproterozoic accretionary complex of the Svecofennian Orogen are quite different, as well as their spatial relationships.

5.5. The relationships between seismogeological models of the crust and upper mantle and models of subhorizontal velocity-density layering of the Earth's crust

As shown above, seismogeological models demonstrate associations of geological bodies of different morphology: inclined and horizontal layers and tectonic sheets, as well as nearly isometric bodies. The velocity-density models obtained with refraction seismic profiling in combination with gravity measurements demonstrate subhorizontal layering of geological medium, which forms in direct connection with the recent state of the crust including actual distribution of lithostatic loading, heat flow, tectonic stresses, and other features. Under the influence of increasing lithostatic load with depth, the density of rocks progressively increases as the variability of the rock density decreases. Importantly, these changes in properties of the crust are reversible. A high level of rock compaction cannot be explained by present ideas concerning metamorphism and/or compaction of rocks based on the results of laboratory study of the rock samples and related numerical models. This implies that additional vigorous mechanisms ensure reversible alteration of rocks. Understanding of these mechanisms is, in our opinion, a promising task for future research. The detailed pattern of density layering indicates displacements in the crust, which deform isodensity surfaces, including the surface of the velocity–density Moho discontinuity. Stepwise bends of isodensity surfaces are distinctly related to previously formed tectonic deformation zones. These bends apparently arose after termination of lithostatic compaction of rocks. The arrangement of dislocations shows that relaxation of recent stresses in the crust occurs as a result of remobilization of older tectonic zones.

We arrive at conclusions of supra-regional significance also.

(i) Nearly horizontal density layering of the continental crust is superposed on previously formed geological structure; the features of this layering are primarily controlled by the recent state of the crust and disturbed by the youngest deformations.

(ii) Interpretations of the lower continental crust as a reflectivity zone and as a layer of elevated density are not completely equivalent. The lower crust is overall manifestly the deepest and the densest element of the subhorizontal density layering of the continental crust, where degree of compaction can cardinally differ from laboratory estimates of relationships between composition of rocks, their density, and velocity. In turn, the seismic image of the reflectivity zone is related to quite definite and space-constrained geological phenomena: magmatic under- and intraplating under conditions of extensional rifting and ascent of mantle plumes, which form the granulite–basic type of the lower crust.

(iii) The high level of rock compaction in the crust under lithostatic loading cannot be explained in terms of metamorphism and/or compaction of rocks based on laboratory investigations of rock samples and numerical modeling. This indicates that additional and very powerful mechanisms exist, which ensure reversible alteration of rocks. Special studies are needed for ascertaining their nature.

5.6. A model of the origin and geodynamic evolution of the Svecofennian Accretionary Orogen: Approaches to creation of models of the Palaeoproterozoic evolution of Lauroscandia, genesis and evolution of the Atlantic Tectonic Zone

Consideration of the 3D model led us to a series of new important observations concerning the structure and evolution of the Palaeoproterozoic Svecofennian Accretionary Orogen.

(i) The accretionary complex is characterized by inclined tectonic delamination. The tectonic sheets, about 15 km thick are composed of granitoids and volcanic/sedimentary rocks, including electro-conductive graphite-bearing sediments of enhanced electrical conductivity, which monotonously and consecutively plunge eastward.

(ii) Approaching the lower crust, the tectonic sheets of the accretionary complex lose their distinct outlines and are replaced in patterns of seismic reflections with homogeneous acoustically translucent medium, where boundaries of separate sheets are traced only fragmentarily. The crust–mantle boundary is diffuse: transition from crust to mantle is recorded in the gradual disappearance of vaguely drawn boundaries of tectonic sheets and in the gradual transition from the acoustically homogeneous and translucent lower crust to the transparent mantle. Nevertheless, the thorough analysis of structural pattern and MT sounding data make it possible to trace boundaries of separate sheets from surface to the crust–mantle boundary.

(iii) Under the influence of the endogenic heat flow, the accretionary complex undergoes not only high-temperature metamorphism, but also partial melting. Blurring of rock contacts, which initially create contrasts of acoustic impedance, is more probably related to melting and mixing of partial melts. As a result, the rock complex which s variable in composition turns into an acoustically homogeneous medium, which is able to generate only weak and irregularly oriented reflections.

(iv) Development of the Svecofennian Accretionary Orogen along the southwestern margin of the Karelia craton involved northeastward subduction and underthrusting of the thick crustal slices formed by the oceanic, island-arc and back-arc assemblages which was accompanied by overthrusting of the upper-crustal tectonic sheets of the same vergence. The resultant crustal structure has typical features of a convergent orogen with characteristic tectonic wedge development (“crocodile” type structure).

The structural ensemble of consecutively plunging tectonic sheets related to the accretionary complex cardinally distinguishes the Svecofennian Orogen from the Karelia Craton. The important characteristics of this ensemble is structural monotony, which is expressed in approximately equal slope and thickness of tectonic sheets, as well as absence of the attributes which would allow recognition of fragments of former island arcs, interarc basins, and microcontinents. The tectonic sheets similarly lose their unambiguous outlines, when they achieve the level of the lower crust, and then appear as if dissolved in acoustically transparent mantle. It should be noted that the recognition of such fragments on the basis of geological surveying and the limited body of information on deep crustal structure (Lahtinen et al., 2005) is also characterized by significant uncertainty. The marked features of seismic images of the accretionary complex allow us to suggest approximately coeval plunging of tectonic sheets and transformation of the ensemble as a whole into an acoustically homogeneous translucent lower crustal complex.

The detailed model of geodynamic evolution of the Svecofennian Orogen, taking into account the data along seismic profiles of the BABEL project (Korja and Heikkinen, 2005), was presented by Lahtinen et al. (2005). Further involvement of the data on deep structure obtained in project FIRE allowed the same authors, with participation of P. Heikkinen, to expand the model, including the postulates of two collisional orogens: the Lapland–Kola and the Savo–Lapland (Lahtinen et al., 2009). According to the main conclusion of these authors, the central part of Fennoscandia represents a Precambrian cratonic domain comprising deep-seated levels of the thick crust exposed now at surface and underlain by the lithospheric mantle, also significant in thickness. The Palaeoproterozoic crust is considered to be a final product of consecutive accretion, continental collision, and collapse of the orogen. It is asserted that structures of the accretionary orogen have been destroyed, and that only separate fragments of accretionary complex have been retained in peculiar refuges represented by space between collided rigid blocks.

The features of deep crustal structure of the Svecofennian Accretionary Orogen characterized in our paper allow us to enhance and develop the existing models of the geodynamic settings and history of the orogen. To prove validity for the model, it is necessary to explain a series of important features of the crust and the crust–mantle boundary of the Svecofennian Orogen:

(i) Evidence for existence of the Palaeoproterozoic juvenile crust formed between 2.2–2.1 Ga and 1.9 Ga and of the Archaean component in the lithosphere, which has been established in the magmatic source of the accretionary complex within the time interval from ~1.90 Ga to 1.87–1.82 Ga.
(ii) High velocity and short-term formation of monotonously plunging tectonic sheets of the accretionary complex as a whole within the time interval between 1.90 Ga and 1.87–1.82 Ga.
(iii) Similar-type and synchronous reorganization of tectonic sheets of the accretionary complex plunging into the mantle.
(iv) Retention of the rock complex belonging to a passive margin in the frontier zone of the Karelia Craton in the absence of appreciable evidence for magmatism inherent for active margins;
(v) Origin of CFGC.

The complex and event-rich Palaeoproterozoic evolution of the eastern part of Fennoscandia was accompanied by short-term and insignificantly scaled ruptures of the continental lithosphere in the inner domain of the Archaean Kola–Karelia continent, which, in turn, was a constituent of the vast Archaean continent of Lauroscandia combining North American and East European cratons. According to several papers (Mints et al., 2010, 2015; Mints and Eriksson, 2016), Lauroscandia could have been a part of the large supercontinent or one of several vast continents stable in the Neoarchaean and Palaeoproterozoic. A reconstruction of the Palaeoproterozoic (~2.5 Ga to ~1.8 Ga) Lauro-Russian intracontinental oval-concentric orogen that encompassed the predominant part of Lauroscandia, and its evolution are shown in Fig. 9. It was supposed that at 2.5 Ga the Lauro-Russian orogen was a large (~3000 km in diameter) oval-shaped intracontinental tectonic ensemble of regional rank (Fig. 9a). Punctuated tectonic and metamorphic evolution of the orogen continued up to ~1.9 Ga. The orogen involved granulite-gneiss complexes, derivatives of juvenile but crust-contaminated mafic magmas (gabbroanorthosites and layered mafic-ultramafic rocks), intrusions of dry high-temperature within-plate granites, enderbites, and charnockites, and low-grade sedimentary-volcanic belts. Emplacement of the granulite-gneiss complexes indicates significant vertical displacements of the deep crustal associations to a higher level in the crust or directly to the erosion level. Most high-temperature granulite-gneiss belts and low-grade sedimentary-volcanic belts form more or less clearly defined arcuate zones. The plume-initiated tectonic events, such as rifting with local transition to spreading and the formation of short-lived oceans that did not lead to the final separation of the supercontinent fragments, can be classified as unsuccessful attempts to break up the Archaean supercontinent (Mints, 2007).

An exception, especially important in respect of the considered problem, is recorded in the origin of the Svecofennian Ocean during the time interval from ~2.2 Ga to 1.9 Ga (Kontinen, 1987; Peltonen et al., 1996, 1998; Buchan et al., 1998; Hanski et al., 1998). Similarly, the study of the eastern margin of North America resulted in reconstruction of the Pre-Labradorian Ocean (Fig. 9b). The closure of this ocean at 1.89–1.83 Ga was accompanied by formation of the Pre-Labradorian and Penokean Accretionary orogens at the eastern margin of the North American Craton (Gower and Krogh, 2002; Schulz and Cannon, 2007) (Fig. 9c). The coexistence of the approximately age-equivalent Svecofennian and Pre-Labradorian oceans suggests complete division of the Archaean continent of Lauroscandia into East European and East American constituents in the second half of the Palaeoproterozoic (Mints, 2014, 2017, 2018; Mints and Eriksson, 2016 and references therein). The subsequent mirror-symmetric formation of Svecofennian and Pre-Labradorian Accretionary orogens along margins of this ocean allows the suggestion of its complete closure and the restoration of united Lauroscandia (Fig. 9d). Thus, the Meso- to Palaeoproterozoic lithosphere, which comprises fragments of the Archaean crust, apparently was formed due to breakup of Lauroscandia and origin of the intercontinental Svecofennian–Pre-Labradorian Ocean between 2.2–2.1 Ga and ~1.9 Ga. The repeated division and following reconstruction of Lauroscandia in the Proterozoic and Phanerozoic geological record suggest existence of a special Atlantic zone. According to Mints and Afonina (2018), the

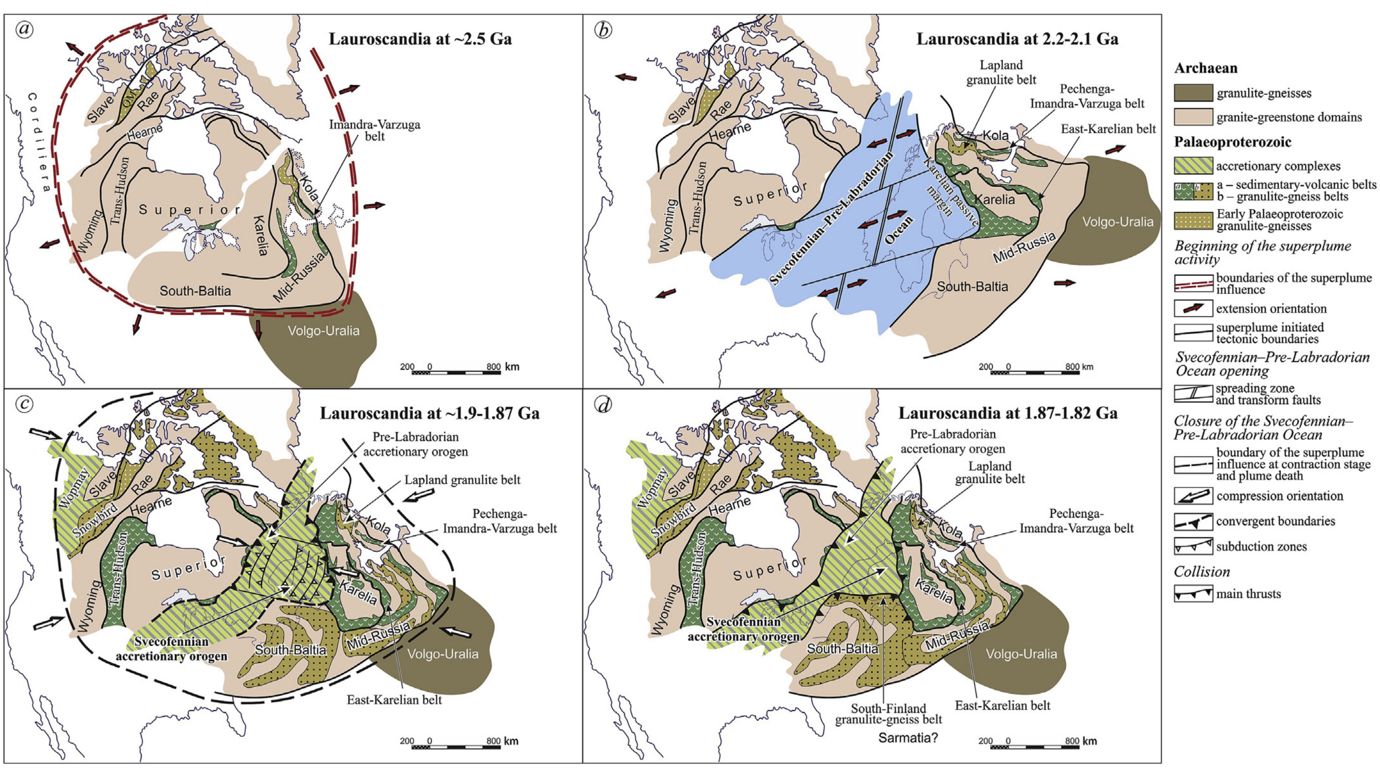

Fig. 9. Model of the Palaeoproterozoic evolution of the intracontinental Lauro-Russian orogen with special attention to the history of the Svecofennian accretionary orogen (after Mints and Eriksson, 2016). The width of the Svecofennian–Pre-Labradorian Ocean is conventional and most likely corresponds to the minimal estimate.

Atlantic Tectonic Zone (Northern and, probably, Southern Atlantic) comprises basement of the present-day Atlantic Ocean and tectonic structures in its framework. The geodynamic settings of their formation are immediately related to initiation and evolution of the Atlantic and preceding oceans. The long-lived (at least, from ~2.2 Ga to the present) Atlantic Tectonic Zone underwent several oceanic openings dated at 2.2–1.8 Ga (Svecofennian Ocean), 1.7–1.3 Ga (Pre-Grenville Ocean), 0.65–0.40 Ga (Iapetus), 0.16 Ga–the Present (Atlantic Ocean). The Atlantic type of geodynamic evolution has been initiated by activity of mantle plumes and exemplifies interaction of plume- and plate-tectonics. It is important to note that the deep-seated links (roots) between separated continental fragments are retained despite faulting of the lithosphere (Goodwin, 1985; O'Reilly et al., 2009). To appraise the degree of uniqueness of this type of evolution and its possible repetation in other regions, including those devoid of present-day oceans, further studies are required.

Intrusion of postkinematic granitoids within CFGC and in its framework 1.89–1.87 Ga ago (Nironen et al., 2000; Rämö et al., 2001) and formation of the South Finland Thrust Belt (Fig. 9d), which ended between 1.87 Ga and 1.82 Ga (Väisänen et al., 2000 and references therein), may be regarded as estimates of the upper age boundary in the history of the accretionary complex. Integrating these estimates, we conclude a short-term and high-rate formation of the accretionary complex during only 30–50 Myr.

The high rate of accretion is confirmed by the similar gradual transition of structurally expressed accretionary complex via acoustically translucent homogeneous lower crustal domain to acoustically transparent mantle over extended sections and by diffuse appearance of the crust–mantle boundary. In contrast to diverse metamorphic or magmatic events, which may have reworked the accretionary complex, the similarity of the results indicates their temporal closeness. The high rate of accretion might be achieved either by fast subsidence of the oceanic lithosphere in a single subduction zone or by a number of synchronously functioning subduction zones. Taking into account the significant extent of the accretionary complex and inferred synchronous origin and absorption of tectonic sheets making up this complex, the second version seems to be preferable.

However, what type of process could be responsible for overall transformation of an accretionary complex at the intersection of the crust–mantle boundary by tectonic sheets? According to the model of Kukkonen et al. (2008), the P–T conditions, which ensure eclogitization of the plunging tectonic sheets, were created at the base of the Svecofennian Orogen due to subduction beneath and collision with the Karelia Craton. It was suggested that the lower part of the eclogitic layer delaminated; the eclogitized rocks of the accretionary complex plunged into the mantle and underwent disintegration. In our view, this model has weak points, which make its application doubtful. First, the high-velocity and high-density crust of the Svecofennian Orogen is traced without any complication beneath the adjacent Karelia Craton, where such important features of the model as the rock composition, temperature and pressure at the base of crust and mechanical properties have to be dramatically changed. Secondly, the heterogeneous accretionary complex consisting of volcanic rocks of different compositions, sedimentary rocks, mafic and granitic intrusive bodies undoubtedly suggests that these rocks, being subject to eclogite facies metamorphism, will keep various density, velocity, and corresponding acoustic impedance characteristics. The contacts of rocks, the eclogitized varieties of which differ in acoustic impedance, will remain sources of seismic reflections. Thus, the eclogite facies metamorphism cannot be a sufficient cause of the medium homogenization and disappearance of the reflection sources. Thirdly, similar seismic images of the crust and crust–mantle boundary were earlier described beyond the Svecofennian Accretionary Orogen, e.g., at the base of the Onega Depression on the Karelia Craton and at the base of the Tokmovo ovoid in the Volgo–Uralia Craton. Taking into consideration the determinant role of mantle-plume processes in the Palaeoproterozoic geodynamics of the East European Craton (Mints et al., 2010 (Chapters 4 and 8), 2015 (Chapters 12 and 14); Mints, 2011, 2016; Mints and Eriksson, 2016, it may be suggested that rocks of the Svecofennian accretionary complex under the effect of endogenic heat flow were subject to partial melting and high-temperature granulite-, and with increase in depth, high-temperature eclogite facies metamorphism (Kukkonen et al., 2008; Glaznev et al., 2015). Furthermore, it may be suggested that partial melting gives rise to blurring of the rock contacts, which created contrasts of acoustic impedance at initial stages. As a result, the complex of rocks was transformed into an acoustically homogeneous medium, which is able to generate only weak and irregularly oriented reflections. With transition to deep levels and due to increase in intensity of magmatic and metamorphic processes, the rocks gradually become acoustically transparent and similar to mantle rocks in this quality. The same changes of acoustic properties are characteristic of the lower crust and crust–mantle boundary at the base of sedimentary basins and of rifts of various ages. The Neoarchaean Witwatersrand Basin in South Africa (De Wit and Tinker, 2004), the Valencia Trough in the western Mediterranean region (Collier et al., 1994), the Palaeozoic sedimentary basin in northeastern Germany (Krawczyk et al., 1999) are the examples. Conversely, reflection seismics, which characterize the Cenozoic accretionary complex of the North American Cordilleras near Vancouver Island and the Palaeoproterozoic Wopmay Orogen in northwestern Canada, which were not subject to mantle–plume activity, display an extended image of the plunging oceanic plate, which is traced to a depth of no less than 80 km (Van der Velden and Cook, 1999). The real depth of penetration of tectonic sheets of the Svecofennian accretionary complex remains uncertain. It can only be suggested that this depth is constrained. It should be specially noted that seismic images of crust in the Svecofennian Orogen are not overlain and obscured with any transformations, which might be responsible for velocity and density layering of the crust revealed by deep seismic sounding and gravitational density simulation.

One more important feature of the Svecofennian Orogen, which differentiates it from recent and contemporary accretionary complexes, consists in the absence of suprasubduction magmatism at the margin of the Karelia Craton. It is evident that this circumstance alone explains preservation of rocks of passive margin affinity in the frontier zone of the craton. Seemingly there is evidence for a certain genetic link between high rates of opening and closure of ocean and formation of accretionary complex: lack of suprasubduction magmatism in the domain, where its manifestation is the most expected; evidence for high-temperature conditions in the mantle of the domain, where tectonic sheets of accretionary complex are plunging, and evidence for crystallization of postkinematic granitoids of CFGC from dry A-type magma and/or magmas of the charnockite–enderbite series under conditions of granulite facies metamorphism. An event of mantle–plume type may be accepted as a natural cause of these features of accretion as a whole. As was shown earlier, the Palaeoproterozoic evolution of East European and North American cratons, and in general of the continent of Lauroscandia, which combines both cratons, may be presented quite completely and consecutively in terms of the superplume event model, which, in turn, initiated plate-tectonic processes (Mints, 2007; Mints et al., 2010 (Chapter 9), 2015 (Chapter 17); Mints and Eriksson, 2016).

The sequence of events made up the model of origin and geodynamic evolution of the Svecofennian Accretionary Orogen. The model integrates geological and geophysical data presented in this paper, and at the same time takes into consideration the position of the Svecofennian Orogen in the structure and geological history of the intracontinental Lauro-Russian Orogen, which occupies a predominant territory within Lauroscandia (Mints, 2014; Mints et al., 2015 Chapter 17) (Fig. 9). This model characterizes five stages of evolution of the Lauro-Russian Orogen and provides position and stages of evolution of the Svecofennian Orogen:

(1) ~2.5 Ga, start of activity of Palaeoproterozoic superplume: initial stage of evolution of Lauro-Russian Orogen, rifting of Archaean

Craton, formation of riftogenic depressions, under- and intraplating with mafic magmas (Fig. 9a);
(2) 2.2–2.1 Ga, concentration of mantle-plume activity in middle part of Lauroscandia: (i) restrictedly developing rifting in continental domain, (ii) transition from rifting to spreading in axial zone, (iii) subsequent division of North American and East European cratons, and (iv) formation of Svecofennian–Pre-Labradorian Ocean (Fig. 9b);
(3) peak of mantle-plume activity is apparently related to time interval of 1.95–1.90 Ga;
(4) later on (1.90–1.87 Ga) decrease of mantle-plume activity follows: reduction of ocean, significant number of synchronously functioning subduction zones, and formation of accretionary orogens completing closure of the Svecofennian–Pre-Labradorian Ocean (Fig. 9c);
(5) 1.87–1.82 Ga, final Palaeoproterozoic mantle-plume activity: general compression and formation of the intracontinental Lauro-Russian Orogen, including displacement of the South Finland tectonic nappe and formation of granulite-gneiss belt characterized by thrust and nappe structure (Fig. 9d).

Thus, the main feature of the Palaeoproterozoic evolution of the Svecofennian Accretionary Orogen and Lauroscandia, as a whole, consists in the causal link with development of a superplume, one of the elements of which is initialization of significant events of plate-tectonic type. As a result, the Svecofennian and Pre-Labradorian orogens originated in the axial zone of the intracontinental Lauro-Russian Orogen. The deep crustal structure and evolution of the Svecofennian Accretionary Orogen are characterized in this paper. The information on structure and history of the Pre-Labradorian Orogen may be found in the paper published by Mints and Eriksson (2016); this paper also contains necessary bibliography.

The dimensions of the head of the Palaeoproterozoic Lauro-Russian superplume are approximately characterized in Fig. 9: about 3500 km in meridional direction and from 3000 km to 5500 km in latitudinal direction at different stages of evolution; 5500 km likely is a minimal estimate of the greatest dimension. The width of the Svecofennian–Pre-Labradorian Ocean of ~2000 km (Fig. 9b) apparently also corresponds to a minimal value. The diameter of the Lauro-Russian intracontinental collision orogen formed in the Palaeoproterozoic is 3500–4000 km. The most significant temporal intervals in the evolution of the intracontinental orogen (~2.5 Ga and 2.2–1.8 Ga ago) coincide in time with superplume events of global rank (Mints and Eriksson, 2016 and references therein), and the obvious phenomenon of inheritance of main tectonic trends indicates the interrelated character of these events.

The model of evolution of the Lauro-Russian Orogen presented above is in some detail similar to the model of an oval-concentric orogen formed in the crustal region *above* a *mantle plume,* proposed by Van Kranendonk (2010). The idea of this model arose under the influence of analysis of the radar image of the Artemis corona on Venus. Artemis Corona is a 1500 km diameter, nearly circular topographic high, encircled by a deep trough and outer rise, and transected by a central rift valley, complete with transform faults (Fig. 10). Its geometry suggests that it could have resulted from emplacement, inflation, overflow and extensional collapse of a thick magmatic welt derived from melting of an upwelling mantle plume. In this model, continued magmatism led to over-inflation of the corona, and this, combined with conductive heat from the plume, led to gravitational collapse and spreading of its central part. The weight of the erupting plume-derived magmatic welt deflected the surrounding crust downward, which is partly compensated for by an outer forebulge (Van Kranendonk, 2010, and references therein).

It should be noted that the idea of Svecofennian Ocean origination as a result of breakup of Lauroscandia and short-term existence of the North American and East European cratons, which follows by recurring integration with accommodation of Svecofennian Orogen in the space between them, appeared only recently (Mints, 2014; Mints and Eriksson, 2016). Subsequently, a suggestion for the existence of the Svecofennian–Pre-Labradorian Ocean, completed by conjugate formation of the Svecofennian–Pre-Labradorian Accretionary Orogen has been published by Mints (2018). On the other hand, according to the model earlier presented by Hoffman (1989), it is suggested that the vast Palaeoproterozoic Ocean preceded genesis of the Trans-Hudson Orogen, which was formed as a result of collison of two independent continental blocks in the second half of the Proterozoic. The palaeomagnetic data provide evidence for significant displacements of the boundaries of the Trans-Hudson Orogen (Gala et al., 1998; Halls and Heaman, 2000; Symons and Harris, 2000). The Manikewan Ocean, which divided the walls of the future orogen about 1.84 Ga ago, could have reached 4000 km in width. However, evidence for starting the events in the evolution of the Trans-Hudson Orogen (2.6–2.5 Ga ago), which are distinctly limited by the periphery and inner domain of this orogen in its present-day configuration (Bickford et al., 2005; Rayner et al., 2005; Dahl et al., 2006), as well as strict parallelism of orogen boundaries and some other features (Mints and Eriksson, 2016) allow us to suggest that the Trans-Hudson Orogen records a place marking the rupture of formerly continuous continent, the formation of relatively narrow ocean, and the subsequent resumption of the continent. The suprasubduction complexes in the framework of the orogen occur only locally. The recurring origination of the Pre-Grenville (~1.7–1.3 Ga), Iapetus (~0.65–0.40 Ga), and Atlantic (0.16 Ga–present time) oceans within the axial zone of Lauroscandia is of principal significance (Mints and Afonina, 2018).

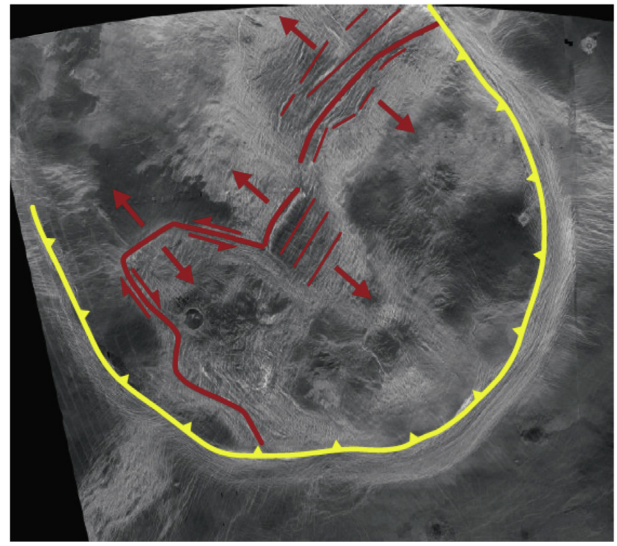

Fig. 10. Annotated synthetic aperture radar image of Artemis Corona, showing central rift valley (heavy red lines, with symmetrical arrows) and linking transform faults (asymmetric red arrows), possible subduction zone on the inner ring of annular trough (yellow line with teeth on upper plate side). Fragment after Van Kranendonk (2010).

Thus, there are sufficient grounds for inferring the similarity between the Trans-Hudson Orogen, on the one hand, and the volcanic-sedimentary belts in the East European Craton, on the other, and for suggestion that the Svecofennian–Pre-Labradorian Ocean played a critical role in fragmentation of the Archaean Lauroscandia.

6. Conclusion

(1) The Early Precambrian crust of the Karelia Craton is characterized by inclined structural layering. The TTG-type crust of the Palaeoarchaean and Mesoarchaean microcontinents within the Karelia Craton and the Belomorian Province are separated by gently dipping greenstone belts, with at least some of them being

palaeosutures. The structure of the crust is mainly determined by the Palaeoproterozoic tectonics in the intra-continental settings.

(2) The crust–mantle boundary, which is apparently a thick zone of tectonic flow and displacement of large crustal sheets, accompanied by the diving of individual lower crustal segments into the mantle.

(3) The main feature of the Palaeoproterozoic evolution of the Svecofennian Accretionary Orogen and Lauroscandia, as a whole, consists in the causal link with development of a superplume, one of the elements of which is initialization of significant events of plate-tectonic type.The evolutionary model of the Svecofennian Orogen includes five stages:
   (i) ~2.5 Ga, start of activity of Palaeoproterozoic superplume;
   (ii) 2.2–2.1 Ga, concentration of mantle-plume activity in middle part of Lauroscandia, formation of Svecofennian–Pre-Labradorian Ocean;
   (iii) 1.95–1.90 Ga, peak of mantle-plume activity;
   (iv) 1.90–1.87 Ga, decrease of mantle-plume activity: reduction of ocean, significant number of synchronously functioning subduction zones, formation of accretionary orogens completing closure of the Svecofennian–Pre-Labradorian ocean;
   (v) 1.87–1.82 Ga, final Palaeoproterozoic mantle-plume activity: general compression and formation of the intracontinental Lauro-Russian Orogen.

(4) The repeated division and following reconstruction of Lauroscandia in the Proterozoic and Phanerozoic geological record suggest existence of a special Atlantic Tectonic Zone.

(5) Seismogeological models based on reflection seismic images demonstrate associations of geological bodies of different morphology, the velocity-density models obtained with refraction seismic profiling in combination with gravity measurements demonstrate subhorizontal layering of geological medium, which forms in direct connection with the recent state of the crust including actual distribution of lithostatic loading, heat flow, tectonic stresses, and other features.

(6) The repeated division and following reconstruction of Lauroscandia in the Proterozoic and Phanerozoic geological record suggest existence of a special Atlantic Tectonic Zone.

(7) Structural characteristics of geological crust–mantle boundary and velocity–density Moho discontinuities at the base of the Archaean Karelian Craton and the Palaeoproterozoic accretionary complex of the Svecofennian Orogen are quite different, as well as their spatial relationships.

(8) The lower crust is overall manifestly the deepest and the densest element of the subhorizontal density layering of the continental crust, where degree of compaction can cardinally differ from laboratory estimates of relationships between composition of rocks, their density, and velocity. In turn, the seismic image of the reflectivity zone is related to quite definite and space-constrained geological phenomena – magmatic under- and intraplating under conditions of extensional rifting and ascent of mantle plumes, which form the granulite–basic type of the lower crust.

(9) Under the influence of increasing lithostatic load with depth, the density of rocks progressively increases as the variability of the rock density decreases. These changes in properties of the crust are reversible. This implies that vigorous mechanisms ensure reversible alteration of rocks. The high level of rock compaction in the crust under lithostatic loading cannot be explained in terms of metamorphism and/or compaction of rocks based on laboratory investigations of rock samples and numerical modeling. This indicates that additional and very powerful mechanisms exist, which ensure reversible alteration of rocks. Understanding of these mechanisms is, in our opinion, a promising task for future research.

Acknowledgements

The work was performed in the framework of the RF state project (No. 0135-2019-0036) and partly supported by the project (No. 0135-2018-0039) of the Program of the Presidium of the RAS "Fundamental problems of geological and geophysical study of lithospheric processes", section 4. The authors are grateful also to the Russian Foundation for Basic Research for supporting project (No. 19-05-00336). The authors thank two anonymous reviewers, who helped significantly improve the manuscript. Recommendations of Reviewer #2 were especially useful. The authors are very grateful to Patrick G. Eriksson (University of Pretoria), who additionally edited the English text of Russian authors.

References

Abbott, D.H., Mooney, W.D., Van Tongeren, J.A., 2013. The character of the Moho and lower crust within Archaean cratons and the tectonic implications. Tectonophysics 609, 690–705. https://doi.org/10.1016/j.tecto.2013.09.014.

Abramovitz, T., Thybo, H., Berthelsen, A., 1997. Proterozoic sutures and terranes in the southeastern Baltic Shield interpreted from BABEL deep seismic data. Tectonophysics 270, 259–277. https://doi.org/10.1016/S0040-1951(96)002.

Andersson, U.B., Högdahl, K., Sjöström, Bergman, S., 2006. Multistage growth and reworking of the Palaeoproterozoic crust in the Bergslagen area, southern Sweden: evidence from U–Pb geochronology. Geol. Mag. 143 (5), 679–697. https://doi.org/10.1017/S0016756806002494.

Andersson, U.B., Begg, G.C., Griffin, W.L., Högdahl, K., 2011. Ancient and juvenile components in the continental crust and mantle: Hf isotopes in zircon from Svecofennian magmatic rocks and rapakivi granites in Sweden. Lithosphere 3 (6), 409–419. https://doi.org/10.1130/L162.1.

Art, J.G., Barker, F., Peterman, Z.E., Friedman, J., 1978. Geochemistry of gabbro-diorite-tonalite-trondhjemite suite of southwest Finland and its implications for the origin of tonalitic and trondhjemitic magmas. J. Petrol. 19, 289–316.

BABEL Working Group, 1990. Evidence for early Proterozoic plate tectonics from seismic reflection profiles in the Baltic Shield. Nature 348, 34–38. https://doi.org/10.1038/348034a0.

Balling, N., 2000. Deep seismic reflection evidence for ancient subduction and collision zones within the continental lithosphere of northwestern Europe. Tectonophysics 329, 269–300. https://doi.org/10.1016/S0040-1951(00)00199-2.

Baltybaev, ShK., Glebovitskiy, V.A., Kozyreva, I.V., Konopelko, D.L., Levchenkov, O.A., Sedova, I.S., Shuldiner, V.I., 2000. Geology and Petrology of the Svecofennids of Ladoga Lake Area. Publishing House of St. Petersburg State University, St. Petersburg, 200 pp. (in Russian).

Baltybaev, S.K., Levchenkov, O.A., Levsky, L.K., Eklund, O., Kilpeläinen, T., 2006. Two metamorphic stages in the Svecofennian domain: evidence from the isotopic geochronological study of the Ladoga and Sulkava metamorphic complexes. Petrology 14, 266–281. https://doi.org/10.1134/S0869591106030039.

Belousov, V.V., 1960. Development of the Earth and tectogenesis. J. Geophys. Res. 65 (12), 4127–4146.

Berdichevsky, M.N., Dmitriev, V.I., 2008. Models and Methods of Magnetotellurics. Springer, Berlin, p. 564.

Berzin, R.G., Suleimanov, A.K., Zamozhnyaya, N.G., Andryushchenko, YuN., Stupak, V.M., 2001. Geophysical investigations on regional profile 4B. In: Sharov, N.V. (Ed.), Deep Structure and Evolution of the Earth's Crust in the Eastern Fennoscandian Shield: Kem'-Kalevala Profile. Karelian Sci. Center. Russian Academy of Sciences, Petrozavodsk, pp. 39–63 (in Russian).

Bickford, M.E., Mock, T.D., Steinhart III, W.E., Collerson, K.D., Lewry, J.F., 2005. Origin of the Archaean Sask craton and its extent within the Trans-Hudson orogen: evidence from Pb and Nd isotopic compositions of basement rocks and post-orogenic intrusions. Can. J. Earth Sci. 42, 659–684. https://doi.org/10.1139/e04-064.

Biske, N.S., Kolodey, V.A., 2014. Spectroscopy of Raman scattering of graphite from deposits and ore occurrences in Ladoga area. In: Golubev, A.I., Shchitsov, V.V. (Eds.), Geology and Minerals of Karelia, 17, pp. 103–109 (in Russian).

Bock, G., Achauer, U., Alinaghi, A., Ansorge, J., Bruneton, M., Friederich, W., Grad, M., Guterch, A., Hjelt, S.-E., Hyvonen, T., Ikonen, J.-P., Kissling, E., Komminaho, K., Korja, A., Heikkinen, P., Kozlovskaya, E., Nevsky, M.V., Pavlenkova, N., Pedersen, H., Plomerová, J., Raita, T., Riznichenko, O., Roberts, R.G., Sandoval, S., Sanina, I.A., Sharov, N., Tiikkainen, J., Volosov, S.G., Wielandt, E., Wylegalla, K., Yliniemi, J., Yurov, Y., 2001. Seismic probing of Fennoscandian lithosphere. Eos 82 (50), 621–636.

Bogdanova, S.V., 1993. Segments of the east European craton. In: Gee, D.G., Beckholmen, M. (Eds.), EUROPROBE in Jablonna 1991. European Science Foundation, Polish Academy of Sciences, pp. 33–38.

Bogdanova, S.V., Gorbatschev, R., Grad, M., Janik, T., Guterch, A., Kozlovskaya, E., Motuza, G., Skridlaite, G., Starostenko, V., Taran, L., the EUROBRIDGE and POLONAISE Working Groups, 2006. EUROBRIDGE: new insight into the geodynamic evolution of the East European Craton. In: Gee, D.G., Stephenson, R.A. (Eds.), European Lithospheric Dynamics, 32. Geological Society London Memoirs, pp. 599–625.

Buchan, K.L., Mortensen, J.K., Card, K.D., Percival, J.A., 1998. Paleomagnetism and U–Pb geochronology of diabase dyke swarms of Minto block, Superior Province, Quebec, Canada. Can. J. Earth Sci. 35, 1054–1069. https://doi.org/10.1139/e98-054.

Burov, E., Diament, M., 1996. Isostasy, equivalent elastic thickness, and inelastic rheology of continents and oceans. Geology 24, 419–422. https://doi.org/10.1130/0091-7613(1996)024<0419:IEETAI>2.3.CO;2.

Carbonell, R., Levander, A., Kind, R., 2013. The Mohorovičić discontinuity beneath the continental crust: an overview of seismic constraints. Tectonophysics 609, 353–376. https://doi.org/10.1016/j.tecto.2013.08.037.

Cherevatova, M.V., 2010. The Electrical Conductivity of the Lithosphere of the Eastern Part of the Fennoscandian Shield Based on the Results of Two-Dimensional Analysis of the Magnetotelluric Data. Ph.D. thesis. S-Pb State University, St. Petersburg, 118 pp. (in Russian).

Christensen, N.I., Mooney, W.D., 1995. Seismic velocity structure and composition of the continental crust: a global view. J. Geophys. Res. 100 (B6), 9761–9788. https://doi.org/10.1029/95JB00259.

Collier, J.S., Buhl, P., Tome, M., Watts, A.B., 1994. Moho and lower crustal reflectivity beneath a young rift basin: results from a two-ship, wide-aperture seismic-reflection experiment in the Valencia Trough (western Mediterranean). Geophys. J. Int. 118, 159–180.

Conrad, V., 1925. Laufzeitkurven des Tauernbebens vom 28. November, 1923. Mitteilungen der Erdbeben-Kommission der Akademie der Wissenschaften in Wien, Neue Folge, 59 (in German).

Cook, F.A., White, D.J., Jones, A.G., Eaton, D.W.S., Hall, J., Clowes, R.M., 2010. How the crust meets the mantle: lithoprobe perspectives on the Mohorovičić discontinuity and crust–mantle transition. Can. J. Earth Sci. 47, 315–351.

Dahl, P.S., Hamilton, M.A., Wooden, J.L., Foland, K.A., Frei, R., McCombs, J.A., Holm, D.K., 2006. 2480 Ma mafic magmatism in the northern Black Hills, South Dakota: a new link connecting the Wyoming and Superior cratons. Can. J. Earth Sci. 43 (10), 1579–1600. https://doi.org/10.1139/e06-066.

De Wit, M., Tinker, J., 2004. Crustal structures across the central Kaapvaal craton from deep-seismic reflection data. S. Afr. J. Geol. 107, 185–206. https://doi.org/10.2113/107.1-2.185.

Downes, H., Peltonen, P., Mänttäri, I., Sharkov, E.V., 2002. Proterozoic zircon ages from lower crustal granulite xenoliths, Kola Peninsula, Russia: evidence for crustal growth and reworking. J. Geol. Soc. 159, 485–488.

Dyadyura, V.A. (Ed.), 1992. New Methods and Systems of Computer-Aided Processing and Interpretation of Seismic Exploration Information: Collection of Papers of School–Workshop. Association of Designers and Users of Computer Technologies Aimed at Integrated Processing and Interpretation of Geological and Geophysical Data: Geoinformmark, Moscow, 145 pp. (in Russian).

Elliott, B.A., Rämö, O.T., Nironen, M., 1998. Mineral chemistry constraints on the evolution of the 1.88–1.87 Ga post-kinematic granite plutons in the Central Finland granitoid complex. Lithos 45, 109–129. https://doi.org/10.1016/S0024-4937(98)00028-0.

Fountain, D.M., Christensen, N.I., 1989. Composition of the continental crust and upper mantle; A review. In: Pakiser, L.C., Mooney, W.D. (Eds.), Geophysical Framework of the Continental United States: Boulder, Colorado, 172. Geological Society of America Memoir, pp. 711–742. https://doi.org/10.1130/MEM172-p711.

Gala, M.G., Symons, D.T.A., Palmer, H.C., 1998. Geotectonics of the Hanson Lake block, Trans-Hudson orogen, Central Canada: a preliminary paleomagnetic report. Precambrian Res. 90, 85–101. https://doi.org/10.1016/S0301-9268(98)00034-5.

Gautneb, H., Ahtola, T., Eklund, O., Lynch, E., 2016. Graphite in Fennoscandia. In: Conference Paper. Nordic Mining Day PDAC 2016.

Glaznev, V.N., 2003. Complex Geophysical Models of the Lithosphere of Fennoscandia. Apatity, KaeM, 252 pp. (in Russian).

Glaznev, V., Scopenko, G., Smolyaninova, E., Lyakhovsky, V., 1991. Complex Geophysical Model of the Crust for the Baltic Profile. Institute of Seismology University of Helsinki. Report S-25, pp. 107–113.

Glaznev, V.N., Kukkonen, I.T., Raevsky, A.B., Ekkinen, J., 2004. New data on thermal flow in the central part of the Kola peninsula. Dokl. Earth Sci. 396 (4), 512–514.

Glaznev, V.N., Mints, M.V., Muravina, O.M., Raevsky, A.B., Osipenko, L.G., 2015. Complex geological–geophysical 3D model of the crust in the southeastern Fennoscandian Shield: nature of density layering of the crust and the crust–mantle boundary. Geodyn. Tectonophysics 6 (2), 133–170. https://doi.org/10.5800/GT-2015-6-2-0176.

Glebovitsky, V.A. (Ed.), 2005. Early Precambrian of the Baltic Shield. Nauka, St. Petersburg, 711 pp. (in Russian).

Goodwin, A.M., 1985. Rooted Precambrian ring-shields: growth, alignment, and oscillation. Am. J. Sci. 285, 481–531. https://doi.org/10.2475/ajs.285.6.481.

Gower, C.F., Krogh, T., 2002. A U–Pb geochronological review of the Proterozoic history of the eastern Grenville Province. Can. J. Earth Sci. 39, 795–829. https://doi.org/10.1139/e01-090.

Grad, M., Tiira, T., ESC Working Group, 2009. The Moho depth map of the European plate. Geophys. J. Int. 176 (1), 279–292. https://doi.org/10.1111/j.1365-246X.2008.03919.x.

Habibian, B.D., Brasse, H., Oskooi, B., Ernst, T., Sokolova, E., Varentsov, Iv, 2010. The conductivity structure across the Trans-European Suture Zone from magnetotelluric and magnetovariational data modelling. Phys. Earth Planet. Inter. 183 (3), 377–386. https://doi.org/10.1016/j.pepi.2010.08.005.

Halls, H.C., Heaman, L.M., 2000. The paleomagnetic significance of new U–Pb age data from the Molson dyke swarm, Cauchon Lake area, Manitoba. Can. J. Earth Sci. 37, 957–966. https://doi.org/10.1139/e00-010.

Hammer, P.T.C., Clowes, R.M., Cook, F.A., Van der Velden, A.J., Vasudevan, K., 2010. The Lithoprobe trans-continental lithospheric cross sections: imaging the internal structure of the North American continent Canadian. J. Earth Sci. 47, 821–857.

Hanski, E.J., Huhma, H., Lehtonen, M.I., Rastas, P., 1998. 2.0 Ga old oceanic crust in northern Finland. In: Hanski, E., Vuollo, J. (Eds.), International Ophiolite Symposium and Field Excursion, Abstracts, 26. Geological Survey of Finland Special Paper, p. 24.

Hoffman, P.F., 1989. In: Bally, A.W., Palmer, A.R. (Eds.), Precambrian Geology and Tectonic History of North America: an Overview, The Geology of North America. Geological Society of America A, pp. 447–512.

Holliger, K., Levander, A., 1994. Lower crustal reflectivity modeled by rheological controls on mafic intrusions. Geology 22, 367–370. https://doi.org/10.1130/0091-7613(1994)022<0367:LCRMBR>2.3.CO;2.

Hölttä, P., Heilimo, E., Huhma, H., Kontinen, A., Mertanen, S., Mikkola, P., Paavola, J., Peltonen, P., Semprich, J., Slabunov, A., Sorjonen-Ward, P., 2012. The Archaean of the Karelia Province in Finland. Geol. Surv. Finl., Special Paper 54, 21–73.

Hölttä, P., Paavola, J., 2000. P-T-t development of Archaean granulites in Varpaisjärvi area, Central Finland. I. Effects of multiple metamorphism on the reaction history of mafic rocks. Lithos 50, 97–120. https://doi.org/10.1016/S0024-4937(99)00056-0.

Hölttä, P., Huhma, H., Mänttäri, I., Paavola, J., 2000a. P-T-t development of Archaean granulites in Varpaisjärvi area, Central Finland. II. Dating of high-grade metamorphism with the U-Pb and Sm-Nd methods. Lithos 50, 121–136. https://doi.org/10.1016/S0024-4937(99)00055-9.

Hölttä, P., Huhma, H., Mänttäri, I., Peltonen, P., Juhanoja, J., 2000b. Petrology and geochemistry of mafic granulite xenoliths from the Lahtojoki kimberlite pipe, eastern Finland. Lithos 51, 109–133. https://doi.org/10.1016/S0024-4937(99)00077-8.

Hölttä, P., Heilimo, E., Huhma, H., Kontinen, A., Mertanen, S., Mikkola, P., Paavola, J., Peltonen, P., Semprich, J., Slabunov, A., Sorjonen-Ward, P., 2014. The Archaean Karelia and Belomorian provinces, Fennoscandian shield. In: Dilek, Y., Furnes, H. (Eds.), Evolution of Archaean Crust and Early Life. Modern Approaches in Solid Earth Sciences 7. Springer Science+Business Media B.V., pp. 55–102. https://doi.org/10.1007/978-94-007-7615-9_3

Huhma, H., 1986. Sm-Nd, U-Pb and Pb-Pb isotopic evidence for the origin of the early Proterozoic Svecokarelian crust in Finland. Geol. Surv. Finl. Bull. 337, 48.

Huhma, H., Claesson, S., Kinney, P.D., Williams, I.S., 1991. The growth of Early Proterozoic crust: new evidence from Svecofennian detrital zircons. Terra. Nova 3, 175–178. https://doi.org/10.1111/j.1365-3121.1991.tb00870.x.

Janik, T., 2010. Upper lithospheric structure in the central Fennoscandian shield: constraints from P- and S-wave velocity models and VP/VS ratio distribution of the BALTIC wide-angle seismic profile. Acta Geophys. 58 (4), 543–586. https://doi.org/10.2478/s11600-010-0002-0.

Janik, T., Kozlovskaya, E., Heikkinen, P., Yliniemi, J., Silvennoinen, H., 2009. Evidence for preservation of crustal root beneath the Proterozoic Lapland-Kola orogen (northern Fennoscandian shield) derived from P and S wave velocity models of POLAR and HUKKA wide-angle reflection and refraction profiles and FIRE4 reflection transect. J. Geophys. Res. 114, B06308. https://doi.org/10.1029/2008JB005689.

Janutyte, I., Kozlovskaya, E., Majdanski, M., Voss, P.H., Budraitis, M., PASSEQ Working Group, 2014. Traces of the crustal units and the upper-mantle structure in the southwestern part of the East European Craton. Solid Earth 5, 821–836. https://doi.org/10.5194/se-5-821-2014.

Ji, S., Long, C., Martignole, J., Salisbury, M., 1997. Seismic reflectivity of a finely layered granulite-facies ductile shear zone in the southern Grenville Province (Quebec). Tectonophysics 279, 113–133.

Jozwiak, W., 2012. Large scale conductivity pattern in Central Europe and its correlation to deep tectonic structures. Pure Appl. Geophys. 169, 1737–1747. https://doi.org/10.1007/s00024-011-0435-7.

Kähkönen, Y., 1989. Geochemistry and petrology of the metavolcanic rocks of the early Proterozoic Tampere schist belt, southern Finland. Geol. Surv. Finl. Bull. 34, 104 pp.

Kähkönen, Y., 1999. Stratigraphy of the central parts of the Palaeoproterozoic Tampere Schist Belt, southern Finland: review and revision. Bull. Geol. Soc. Finl. 71 (Part 1), 13–29.

Kähkönen, Y., Lahtinen, R., Nironen, M., 1994. Palaeoproterozoic supracrustal belts in southwestern Finland. In: Pajunen, M. (Ed.), High Temperature–Low Pressure Metamorphism and Deep Crustal Structures. Meeting of International Geoscience Programme (IGCP) Project 304 "Deep Crustal Processes" in Finland, 37. Geological Survey of Finland Guide, pp. 43–47.

Koistinen, T., Klein, V., Koppelmaa, H., Korsman, K., Lahtinen, R., Nironen, M., Puura, V., Saltykova, T., Tikhomirov, S., Yanovskiy, A., 1996. Paleoproterozoic Svecofennian orogenic belt in the surroundings of the Gulf of Finland. In: Koistinen, T.J. (Ed.), Explanation to the Map of Precambrian Basement of the Gulf of Finland and Surrounding Area, Scale 1:1,000,000, 21. Geological Survey of Finland Special Paper, pp. 21–57.

Koistinen, T., Stephens, M.B., Bogatchev, V., Nordgulen, I., Wennerström, M., Korhonen, J., 2001. Geological Map of the Fennoscandian Shield. Scale 1 : 2 000 000. Geological Surveys of Finland, Norway and Sweden and the North-West Department of Natural Resources of Russia.

Kontinen, A., 1987. An early Proterozoic ophiolite – the Jormua mafic-ultramafic complex, northeastern Finland. Precambrian Res. 35, 313–341. https://doi.org/10.1016/0301-9268(87)90061-1.

Kontinen, A., 1988. The nature of the serpentinites, associated dolomite-skarn-quartz rocks and massive Co-Cu-Zn sulphide ores in the Outokumpu area, eastern Finland. In: Hanski, E., Vuollo, J. (Eds.), Generation and Emplacement of Ophiolites through Time, International Ophiolite Symposium and Field Excursion, University of Oulu, Oulu, Finland, Abstracts, 26. Geological Survey of Finland Special Paper, p. 33.

Kontinen, A., Paavola, J., 2006. A preliminary model of the crustal structure of the eastern Finland Archaean complex between Vartius and Vieremä, based on constraints from surface geology and Fire 1 seismic survey. In: Kukkonen, I.T., Lahtinen, R. (Eds.), Finnish Reflection Experiment FIRE 2001-2005, 43. Geological Survey of Finland Special Paper, pp. 223–240.

Kontinen, A., Peltonen, P., Huhma, H., 2006. Description and genetic modelling of the Outokumpu-type rock assemblage and associated sulphide deposits. GTK report M 104/2006/1. In: Final Technical Report for GEOMEX J.V., Workpackage "Geology". Geological Survey of Finland, Kuopio and Espoo Units, 378 pp.

Korja, A., Heikkinen, P., 2005. The accretionary Svecofennian orogen – insight from the BABEL profiles. Precambrian Res. 136, 241–268. https://doi.org/10.1029/94TC02905.
Korja, A., Heikkinen, P., 2008. Seismic images of Paleoproterozoic microplate boundaries in Fennoscandian shield. In: Condie, K., Pease, V. (Eds.), When Did Plate Tectonics Begin on Planet Earth?, Vol. 400. Geological Society of America Special Paper, pp. 229–248.
Korja, T., Engels, M., Zhamaletdinov, A.A., Kovtun, A.A., Palshin, N.A., Smirnov, M.Yu, Tokarev, A.D., Asming, V.E., Vanyan, L.L., Vardaniants, I.L., the BEAR Working Group, 2002. Crustal conductivity in Fennoscandia – a compilation of a database on crustal conductance in the Fennoscandian Shield. Earth Planets Space 54, 535–558.
Korja, A., Lahtinen, R., Heikkinen, P., Kukkonen, I.N., FIRE Working Group, 2006a. A geological interpretation of the upper crust along FIRE 1. In: Finnish Reflection Experiment FIRE 2001-2005. Geological Survey of Finland Special Paper, 43, pp. 45–76.
Korja, A., Lahtinen, R., Nironen, M., 2006b. The Svecofennian orogen: a collage of microcontinents and island arcs. In: Gee, D.G., Stephenson, R.A. (Eds.), European Lithosphere Dynamics, 32. Geological Society London Memoirs, pp. 561–578.
Korsman, K., Koistinen, T., Kohonen, J., Wennerström, M., Ekdahl, E., Honkamo, M., Idman, H., Pekkala, Y., 1997. Suomen Kallioperäkartta-Berggrundskarta Över Finland (Bedrock Map of Finland). Espoo, Finland, Geological Survey of Finland, Scale 1:1 000 000.
Korsman, K., Korja, T., Papunen, M., Virransalo, P., GGT/SVEKA Working Group, 1999. The GGT/SVEKA Transect: structure and evolution of the continental crust in the Paleoproterozoic Svecofennian orogen in Finland. Int. Geol. Rev. 41, 287–333. https://doi.org/10.1080/00206819909465144.
Kozlovskaya, E., Elo, S., Hjelt, S.-E., Yliniemi, J., Pirttijärvi, M., SVEKALAPKO Seismic Tomography Working Group, 2004. 3-D density model of the crust of southern and central Finland obtained from joint interpretation of the SVEKALAPKO crustal P-wave velocity models and gravity data. Geophys. J. Int. 158, 827–848. https://doi.org/10.1111/j.1365-246X.2004.02363.x.
Kozlovsky, E.A., 1984. Kola Superdeep. Moscow, Nedra, 490 pp. (in Russian).
Krawczyk, C.M., Stiller, M., DEKORP–BASIN Research Group, 1999. Reflection seismic constraints on Paleozoic crustal structure and Moho beneath the NE German Basin. Tectonophysics 314, 241–253. https://doi.org/10.1016/S0040-1951(99)00246-2.
Kukkonen, I., Lahtinen, R., 2006. Finnish Reflection Experiment FIRE 2001-2005. Geological Survey of Finland Special Paper, Finland, p. 247.
Kukkonen, I.T., Kuusisto, M., Lehtonen, M., Peltonen, P., 2008. Delamination of eclogitized lower crust: control on the crust–mantle boundary in the central Fennoscandian shield. Tectonophysics 457, 111–127. https://doi.org/10.1016/j.tecto.2008.04.029.
Kuusisto, M., Kukkonen, I.T., Heikkinen, P., Pesonen, L.J., 2006. Lithological interpretation of crustal composition in the Fennoscandian Shield with seismic velocity data. Tectonophysics 420, 283–299. https://doi.org/10.1016/j.tecto.2006.01.014.
Lahtinen, R., Huhma, H., 1997. Isotopic and geochemical constraints on the evolution of the 1.93–1.79 Ga Svecofennian crust and mantle. Precambrian Res. 82, 13–34. https://doi.org/10.1016/S0301-9268(96)00062-9.
Lahtinen, R., Huhma, H., Kousa, J., 2002. Contrasting source components of the Paleoproterozoic Svecofennian metasediments: detrital zircon U-Pb, Sm-Nd and geochemical data. Precambrian Res. 116, 81–109. https://doi.org/10.1016/S0301-9268(02)00018-9.
Lahtinen, R., Korja, A., Nironen, M., 2005. Paleoproterozoic tectonic evolution. In: Lehtinen, M., Nurmi, P.A., Rämö, O.T. (Eds.), Precambrian Geology of Finland – Key to the Evolution of the Fennoscandian Shield. Elsevier B.V., Amsterdam, pp. 481–532.
Lahtinen, R., Korja, A., Nironen, M., Heikkinen, P., 2009. Palaeoproterozoic accretionary processes in Fennoscandia. In: Cawood, P.A., Kröner, A. (Eds.), Earth Accretionary Systems in Space and Time, 318. Geol. Soc. Lond. Spec. Publ, pp. 237–256. https://sp.lyellcollection.org/content/318/1/237.
Lahtinen, R., Huhma, H., Lahaye, Y., Kousa, J., Luukas, J., 2015. Archaean–Proterozoic collision boundary in central Fennoscandia: revisited. Precambrian Res. 261, 127–165. https://doi.org/10.1016/j.precamres.2015.02.012.
Lyakhovsky, V., Ben-Zion, Y., 2009. Evolving geometrical and material properties of fault zones in a damage rheology model. Geochem. Geophys. Geosyst. 10 (11), 1–13. https://doi.org/10.1029/2009GC002543.
McBride, J.H., White, R.S., Smallwood, J.R., England, R.W., 2004. Must magmatic intrusion in the lower crust produce reflectivity? Tectonophysics 388, 271–297. https://doi.org/10.1016/j.tecto.2004.07.055.
Meissner, R., Rabbel, W., Kern, H., 2006. Seismic lamination and anisotropy of the lower continental crust. Tectonophysics 416, 81–99. https://doi.org/10.1016/j.tecto.2005.11.013.
Miller, YuV., Baikova, N.A., Arestova, N.A., Shuleshko, I.K., 2005. A role of the Khetolambina terrain in the making and early history of development of the Belomorian mobile belt. Geotectonics 2, 17–32 (in Russian).
Mints, M.V., 2007. Paleoproterozoic supercontinent: origin and evolution of accretionary and collisional orogens exemplified in northern cratons. Geotectonics 41 (4), 257–280. https://doi.org/10.1134/S0016852107040012.
Mints, M.V., 2011. 3D model of deep structure of the early Precambrian crust in the east European craton and paleogeodynamic implications. Geotectonics 45 (4), 267–290. https://doi.org/10.1134/S0016852111040054.
Mints, M.V., 2013. Proterozoic evolution of Lauroscandia (from ~ 2.5 to ~0.85 Ga). In: Veselovskiy, R., Lubnina, N. (Eds.), Rodinia-2013: Supercontinental Cycles and Geodynamics Symposium 2013. PERO Press, Moscow, p. 52.
Mints, M.V., 2014. Tectonics and geodynamics of granulite-gneiss complexes in the east European craton. Geotectonics 48 (6), 498–524. https://doi.org/10.1134/S0016852114060089.
Mints, M.V., 2016. Seismic images of the crust-mantle boundary as an expression of geodynamics of the Precambrian crust formation. Geophys. Res. 17 (1), 65–82 (in Russian).
Mints, M.V., 2017. Meso-Neoproterozoic Grenvill-Sveconorwegian intracontinental orogen: history, tectonics, geodynamics. Geodyn. Tectonophysics 8 (3), 619–642. https://doi.org/10.5800/GT-2017-8-3-0309 (in Russian).
Mints, M.V., 2018. 3D model of the deep structure of the Svecofennian Accretionary Orogen: a geodynamic interpretation. series “Geology of Precambrian” Trans. Karelian Res. Cent. Russ. Acad. Sci. 2, 62–76. https://doi.org/10.17076/geo698 (in Russian).
Mints, M.V., Afonina, T.B., 2018. Atlantic Tectonic Zone: plate tectonics initiated by superplume. Geosci. Sci. J. 1, 12–34 (in Russian). http://geo-science.ru/wp-content/uploads/GeoScience-1-2018-012-034-1.pdf.
Mints, M.V., Eriksson, P.G., 2016. Secular changes in relationships between plate-tectonic and mantle-plume engendered processes during Precambrian time. Geodyn. Tectonophysics 7 (2), 173–232. https://doi.org/10.5800/GT-2016-7-2-0203.
Mints, M.V., Sokolova, E.Yu, LADOGA Working Group, 2018. 3D model of the deep structure of the Svecofennian Accretionary Orogen based on data from CDP seismic reflection method, MT sounding and density modeling. a series "Geology of Precambrian Trans. Karelian Res. Cent. Russ. Acad. Sci. 2, 34–61. https://doi.org/10.17076/geo656 (in Russian).
Mints, M.V., Stupak, V.M., 2001. Methodical approaches to geological interpretation of the seismic data characterizing deep structure of the crystalline crust along the 4B profile. In: Sharov, N.V. (Ed.), Deep Structure and Evolution of the Earth’s Crust in the Eastern Fennoscandian Shield: Kem–Kalevala Profile. Karelian Science Center, Russian Academy of Sciences, Petrozavodsk, pp. 144–156 (in Russian).
Mints, M.V., Kolpakov, N.I., Lanev, V.S., Rusanov, M.S., 1987a. The character of the subhorizontal seismic boundaries within the upper part of the Earth’s crust (according to data from the Kola Ultradeep Well). Geotectonics 21 (5), 443–451.
Mints, M.V., Kolpakov, N.I., Lanev, V.S., Rusanov, M.S., Lyakhovsky, V.A., Myasnikov, V.P., 1987b. On the problem of the nature of subhorizontal seismic boundaries (interpretation of Kola super-deep hole). Doklady. Acad. Sci. USSR. 296 (1), 71–76 (in Russian).
Mints, M.V., Glaznev, V.N., Raevsky, A.B., 1995. Three-dimensional geological model of the geological structure of the Earth’s upper crust, the Kola ultradeep borehole and adjacent areas of the Kola Peninsula. Geotectonics 6, 457–475.
Mints, M.V., Glaznev, V.N., Konilov, A.N., Kunina, N.M., Nikitichev, A.P., Raevsky, A.B., Sedykh, YuN., Stupak, V.M., Fonarev, V.I., 1996. Early Precambrian of the Northeastern Baltic Shield: Paleogeodynamics, Crustal Structure and Evolution. Scientific World, Moscow, 287 pp. (Transactions of GIN RAS 503) (in Russian with English abstract).
Mints, M.V., Berzin, R.G., Suleimanov, A.K., Zamozhnyaya, N.G., Stupak, V.M., Konilov, A.N., Zlobin, V.L., Kaulina, T.V., 2004. The deep structure of the Early Precambrian crust of the Karelia craton, southeastern Fennoscandian Shield: results of investigation along CMP profile 4B. Geotectonics 38 (2), 10–29.
Mints, M.V., Kaulina, T.V., Konilov, A.N., Krotov, A.V., Stupak, V.M., 2007. The thermal and geodynamic evolution of the Lapland granulite belt: implications for the thermal structure of the lower crust during granulite-facies metamorphism. Gondwana Res. 12 (3), 252–267.
Mints, M., Suleimanov, A., Zamozhniaya, N., Stupak, V., 2009. A 3-D model of the early Precambrian crust under the southeastern Fennoscandian shield: Karelia craton and belomorian tectonic province. Tectonophysics 472 (1–4), 323–339. https://doi.org/10.1016/j.tecto.2008.12.008.
Mints, M.V., Suleimanov, A.K., Babayants, P.S., Belousova, E.A., Blokh, YuI., Bogina, M.M., Bush, W.A., Dokukina, K.A., Zamozhniaya, N.G., Zlobin, V.L., Kaulina, T.V., Konilov, A.N., Mikhailov, V.O., Natapov, L.M., Piip, V.B., Stupak, V.M., Tihotsky, S.A., Trusov, A.A., Philippova, I.B., Shur, D.Yu, 2010. Deep Crustal Structure, Evolution and Mineral Deposits of the Early Precambrian Basement of the East European Craton: Interpretation of the Data along the 1-EU Geotraverse, the 4B and TATSEIS Profiles, 1. GEOKART, GEOS, Moscow vol. 2, p. 408.
Mints, M.V., Dokukina, K.A., Konilov, A.N., Philippova, I.B., Zlobin, V.L., Babayants, P.S., Belousova, E.A., Blokh, YuI., Bogina, M.M., Bush, W.A., Dokukin, P.A., Kaulina, T.V., Natapov, L.M., Piip, V.B., Stupak, V.M., Suleimanov, A.K., Trusov, A.A., Van, K.V., Zamozhniaya, N.G., 2015. East European Craton: early Precambrian history and 3D models of deep crustal structure. Geol. Soc. Am. Spec. Pap. 510, 433. https://doi.org/10.1130/2015.2510.
Mooney, W.D., Meissner, R., 1992. Multi-genetic origin of crustal reflectivity: a review of seismic reflection profiling of the continental lower crust and Moho. In: Fountain, D.M., Arculus, R., Kay, R.W. (Eds.), Continental Lower Crust. Elsevier, Amsterdam, pp. 45–79.
Mooney, W.D., Prodehl, C., Pavlenkova, N.I., 2002. Seismic velocity structure of the continental lithosphere from controlled source data (Chapter 54). In: Lee, W.H.K., Kanamori, H., Jennings, P., Kisslinger, C. (Eds.), International Handbook of Earthquake and Engineering Seismology 81A, pp. 887–910.
Nikkilä, K., Mänttäri, I., Nironen, M., Eklund, O., Korja, A., 2016. Three stages to form a large batholith after terrane accretion – an example from the Svecofennian orogen. Precambrian Res. 281, 618–638.
Nironen, M., 2017. Bedrock of Finland at the scale 1:1 000 000-major stratigraphic units, metamorphism and tectonic evolution. Geol. Surv. Finl. Special Paper 60, 128.
Nironen, M., Elliott, B.A., Rämö, O.T., 2000. 1.88-1.87 Ga post-kinematic intrusions of the Central Finland Granitoid Complex: a shift from C-type to A-type magmatism during

lithospheric convergence. Lithos 53, 37–58. https://doi.org/10.1016/S0024-4937(00)00007-4.

O'Reilly, S.Y., Griffin, W.L., 2013. Moho vs crust–mantle boundary: evolution of an idea. Tectonophysics 609, 535–546. https://doi.org/10.1016/j.tecto.2012.12.031.

O'Reilly, S.Y., Zhang, M., Griffin, W.L., Begg, G., Hronsky, J., 2009. Ultradeep continental roots and their oceanic remnants: a solution to the geochemical "mantle reservoir" problem? Lithos 211, 1043–1054. https://doi.org/10.1016/j.lithos.2009.04.028.

Pajunen, M., Airo, M., Elminen, T., Mänttäri, I., Niemelä, R., Vaarma, M., Wasenius, P., Wennerström, M., 2008. Tectonic evolution of the Svecofennian crust in southern Finland. In: Pajunen, M. (Ed.), Tectonic Evolution of the Svecofennian Crust in Finland - a Basis for Characterizing Bedrock Technical Properties. Geological Survey of Finland, pp. 15–160. Special Paper 47. http://tupa.gtk.fi/julkaisu/specialpaper/sp_047.pdf.

Pajunpää, K., 1987. Conductivity anomalies in the baltic shield in Finland. Geophys. J. R. Astron. Soc. 91, 657–666. https://doi.org/10.1111/j.1365-246X.1987.tb01663.x.

Peltonen, P., Mänttäri, I., Huhma, H., Whitehouse, M.J., 2006. Multi-stage origin of the lower crust of the Karelian craton from 3.5 to 1.7 Ga based on isotopic ages of kimberlite-derived mafic granulite xenoliths. Precambrian Res. 147, 107–123. https://doi.org/10.1016/j.precamres.2006.02.008.

Peltonen, P., Kontinen, A., Huhma, H., 1996. Petrology and geochemistry of metabasalts from the 1.95 Ga Jormua ophiolite, northeastern Finland. J. Petrol. 37, 1359–1383. https://doi.org/10.1093/petrology/37.6.1359.

Peltonen, P., Kontinen, A., Huhma, H., 1998. Petrogenesis of the mantle sequence of the Jormua Ophiolite (Finland): melt migration in the upper mantle during Palaeoproterozoic continental break-up. J. Petrol. 39, 297–329. https://doi.org/10.1093/petroj/39.2.297.

Prodehl, C., Kennett, B., Artemieva, I., Thybo, H., 2013. 100 years of seismic research on the Moho. Tectonophysics 609, 9–44. https://doi.org/10.1016/j.tecto.2013.05.036.

Rämö, O.T., Vaasjoki, M., Mänttäri, I., Elliott, B.A., Nironen, M., 2001. Petrogenesis of the post-kinematic magmatism of the Central Finland Granitoid Complex: I. Radiogenic isotope constraints and implications for crustal evolution. J. Petrol. 42, 1971–1993. https://doi.org/10.1093/petrology/42.11.1971.

Rayner, N.M., Stern, R.A., Bickford, M.E., 2005. Tectonic implications of new SHRIMP and TIMS U–Pb geochronology of rocks from the Sask craton, Peter Lake Domain, and Hearne margin, Trans-Hudson orogen, Saskatchewan. Can. J. Earth Sci. 42 (4), 635–657. https://doi.org/10.1139/e04-045.

Rebetsky, Y.L., 2007. Tectonic Stress and Strength of Natural Massive. Publishing House Akademkniga, 406 pp. (in Russian).

Rutland, R.W.R., Williams, I.S., Korsman, K., 2004. Pre-1.91 Ga deformation and metamorphism in the Palaeoproterozoic Vammala migmatite belt, southern Finland, and implications for Svecofennian tectonics. Bull. Geol. Soc. Finl. 76 (1–2), 93–140.

Schulz, K.J., Cannon, W.F., 2007. The Penokean orogeny in the Lake Superior region. Precambrian Res. 157, 4–25. https://doi.org/10.1016/j.precamres.2007.02.022.

Silvennoinen, H., Kozlovskaya, E., Kissling, E., Kosarev, G., the POLENET/LAPNET Working Group, 2014. A new Moho boundary map for the northern Fennoscandian Shield based on combined controlled-source seismic and receiver function data. GeoResJ 1–2, 19–32. https://doi.org/10.1016/j.grj.2014.03.001.

Slabunov, A.I., Lobach-Zhuchenko, S.B., Bibikova, E.V., Balagansky, V.V., Sorjonen-Ward, P., Volodichev, O.I., Shchipansky, A.A., Svetov, S.A., Chekulaev, V.P., Arestova, N.A., Stepanov, V.S., 2006. The Archaean of the Baltic shield: geology, geochronology, and geodynamic settings. Geotectonics 40 (6), 409–433. https://link.springer.com/article/10.1134%2FS001685210606001X.

Sorjonen-Ward, P., Ord, A., Kontinen, A., Alt-Epping, P., Zhang, Y., Kuronen, U., 2004. Geological constraints and numerical simulations of the formation and deformation of the Outokumpu Cu–Co–Ni–Zn–Au deposits. In: Predictive Mineral Discovery under Cover, SEG Meeting, Perth, Western Australia, Centre for Global Metallogeny, University of Western Australia, Extended Abstracts, 33, pp. 285–288.

Stepanova, A.V., Samsonov, A.V., Salnikova, E.B., Puchtel, I.S., Larionova, YuO., Larionov, A.N., Stepanov, V.S., Shapovalov, Y.B., Egorova, S.V., 2014. Palaeoproterozoic continental MORB-type tholeiites in the Karelian craton: petrology, geochronology, and tectonic setting. J. Petrol. 55 (9), 1719–1751. https://doi.org/10.1093/petrology/egu039.

Stupak, V.M., 2000. Differential seismic exploration as a tool for scrutiny of geological section. In: Unconventional Methods of Prospecting for Mineral Deposits: St. Petersburg, pp. 164–176 (in Russian).

Symons, D.T.A., Harris, M.J., 2000. The ~1830 Ma Trans-Hudson hairpin from paleomagnetism of the Wapisu gneiss dome, Kisseynew domain, Manitoba. Can. J. Earth Sci. 37, 913–922. https://doi.org/10.1139/e99-043.

Tesauro, M., Kaban, M., Cloetingh, S., 2008. EuCRUST-07: a new reference model for the European crust. Geophys. Res. Lett. 35, L05313. https://doi.org/10.1029/2007GL032244.

Thybo, H., Artemieva, I.M., 2013. Moho and magmatic underplating in continental lithosphere. Tectonophysics 609, 605–619. https://doi.org/10.1016/j.tecto.2013.05.032.

Väisänen, M., Mänttäri, I., Kriegsman, L.M., Hölttä, P., 2000. Tectonic setting of post-collisional magmatism in the Palaeoproterozoic Svecofennian orogen, SW Finland. Lithos 54, 63–81. https://doi.org/10.1016/S0024-4937(00)00018-9.

Vaittinen, K., Korja, T., Kaikkonen, P., Lahti, I., Smirnov, M.Yu, 2012. High-resolution magnetotelluric studies of the Archaean–Proterozoic border zone in the Fennoscandian Shield, Finland. Geophys. J. Int. 188, 908–924. https://doi.org/10.1111/j.1365-246X.2011.05300.x.

Van der Velden, A.J., Cook, F.A., 1999. Proterozoic and Cenozoic subduction complexes: a comparison of geometric features. Tectonics 18 (4), 575–581. https://doi.org/10.1029/1999TC900011.

Van der Velden, A.J., Cook, F.A., 2005. Relict subduction zones in Canada. J. Geophys. Res. 110, B08403. https://doi.org/10.1029/2004JB003333.

Van Kranendonk, M.J., 2010. Two types of Archaean continental crust: plume and plate tectonics on early Earth. Am. J. Sci. 310, 1187–1209. https://doi.org/10.2475/10.2010.01.

Vasiliev, S.A., Urupov, A.K., 1978. New possibilities for studying seismic wave velocity and medium structure from observations at reciprocal points. Nedra, Moscow Appl. Geophys. 92, 3–16 (in Russian).

Vetrin, V.R., 2006. Composition and structure of the lower crust of the Belomorian Mobile Belt, Baltic Shield. Petrology 14 (4), 415–438. https://doi.org/10.1134/S0869591106040047.

Vetrin, V.R., Lepekhina, E.N., Paderin, I.P., Rodionov, N.V., 2009. Stages of the lower crust formation of the Belomorian Mobile Belt, Kola Peninsula. Dokl. Earth Sci. 425, 269–273. https://doi.org/10.1134/S1028334X09020214.

Vetrin, V.R., Belousova, E.A., Kremenetsky, A.A., 2018. Lu–Hf isotopic systematics of zircon from lower crustal xenoliths in the Belomorian Mobile Belt. Geol. Ore Deposits 60 (7), 568–577. https://doi.org/10.1134/S1075701518070085.

Weckmann, U., 2012. Making and breaking of a continent: following the scent of geodynamic imprints on the African continent using electromagnetics. Surv. Geophys. 33, 107–134. https://doi.org/10.1007/s10712-011-9147-x.

White, D.J., Forsyth, D.A., Asudeh, I., Carr, S.D., Wu, H., Easton, R.M., Mereu, R.F., 2000. A seismic-based cross-section of the Grenville Orogen in southern Ontario and western Quebec. Can. J. Earth Sci. 37, 183–192. https://doi.org/10.1139/e99-094.

White, D.J., Thomas, M.D., Jones, A.G., Hope, J., Németh, B., Hajnal, Z., 2005. Geophysical transect across a Paleoproterozoic continent–continent collision zone: the Trans-Hudson Orogen. Can. J. Earth Sci. 42, 385–402. https://doi.org/10.1139/E05-002.

Yin, Y., Unsworth, M., Liddell, M., Pana, D., Craven, J.A., 2014. Electrical resistivity structure of the Great Slave Lake shear zone, northwest Canada: implications for tectonic history. Geophys. J. Int. 199, 178–199. https://doi.org/10.1093/gji/ggu251.

Zhamaletdinov, A.A., Kulik, S.N., 2012. The largest anomalies in the electrical conductivity of the world. Geophys. J. 34 (4), 22–39 (in Russian).